New Global Insights on the Regulation of the Biphasic Life Cycle and Virulence *Via* ClpP-Dependent Proteolysis in *Legionella pneumophila*

Authors

Zhenhuang Ge, Peibo Yuan, Lingming Chen, Junyi Chen, Dong Shen, Zhigang She, and Yongjun Lu

Correspondence

luyj@mail.sysu.edu.cn

Graphical Abstract

In Brief

In this work, we present a comprehensive proteomic profile on the life cycle–dependent proteins that are regulated by ClpP-dependent proteolysis and report the temporal regulation of effector expression *via* the ClpP proteolytic pathway. This study advances our understanding of *Legionella* in response to different conditions for replication and survival and provides additional evidence that the completion of the biphasic life cycle and bacterial pathogenesis is greatly dependent on protein homeostasis mediated by ClpP-dependent proteolysis.
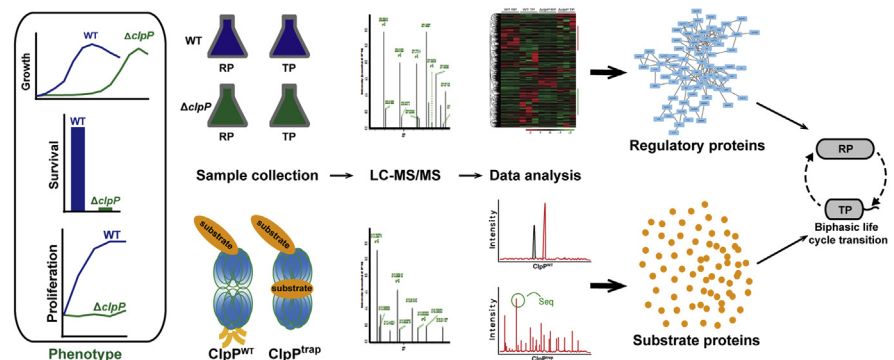
Highlights

- ClpP is the major determinant of biphasic life cycle–dependent protein turnover.
- ClpP-dependent proteolysis monitors SpoT abundance for cellular differentiation.
- ClpP-dependent regulation of life cycle and bacterial virulence is independent.
- ClpP-dependent proteolysis of T4BSS and effector proteins is vital for virulence.

New Global Insights on the Regulation of the Biphasic Life Cycle and Virulence *Via* ClpP-Dependent Proteolysis in *Legionella pneumophila*

Zhenhuang Ge[1,2,3], Peibo Yuan[4], Lingming Chen[5], Junyi Chen[2,3], Dong Shen[2], Zhigang She[1], and Yongjun Lu[2,3,*]

Legionella pneumophila, an environmental bacterium that parasitizes protozoa, causes Legionnaires' disease in humans that is characterized by severe pneumonia. This bacterium adopts a distinct biphasic life cycle consisting of a nonvirulent replicative phase and a virulent transmissive phase in response to different environmental conditions. Hence, the timely and fine-tuned expression of growth and virulence factors in a life cycle–dependent manner is crucial for survival and replication. Here, we report that the completion of the biphasic life cycle and bacterial pathogenesis is greatly dependent on the protein homeostasis regulated by caseinolytic protease P (ClpP)-dependent proteolysis. We characterized the ClpP-dependent dynamic profiles of the regulatory and substrate proteins during the biphasic life cycle of *L. pneumophila* using proteomic approaches and discovered that ClpP-dependent proteolysis specifically and conditionally degraded the substrate proteins, thereby directly playing a regulatory role or indirectly controlling cellular events *via* the regulatory proteins. We further observed that ClpP-dependent proteolysis is required to monitor the abundance of fatty acid biosynthesis–related protein Lpg0102/Lpg0361/Lpg0362 and SpoT for the normal regulation of *L. pneumophila* differentiation. We also found that the control of the biphasic life cycle and bacterial virulence is independent. Furthermore, the ClpP-dependent proteolysis of Dot/Icm (defect in organelle trafficking/intracellular multiplication) type IVB secretion system and effector proteins at a specific phase of the life cycle is essential for bacterial pathogenesis. Therefore, our findings provide novel insights on ClpP-dependent proteolysis, which spans a broad physiological spectrum involving key metabolic pathways that regulate the transition of the biphasic life cycle and bacterial virulence of *L. pneumophila*, facilitating adaptation to aquatic and intracellular niches.

Legionella pneumophila is a Gram-negative and intracellular bacterial pathogen that causes Legionnaires' disease, which is characterized by severe pneumonia in humans [1–4]. This bacterium adopts a biphasic life cycle, which simultaneously allows it to benefit from the environment of the susceptible host cell and to ensure its persistence for another infection cycle [5–7]. In broth cultures and within host cells, the biphasic life cycle alternates between two distinct and reciprocal forms, replicative and transmissive. This process is called microbial differentiation, in which *L. pneumophila* undergoes physiological, morphogenetic, and metabolic changes [7]. For example, when conditions are favorable for multiplication, virulence traits are neither required nor expressed. However, the bacteria will not replicate in adverse conditions (*e.g.*, nutrient deprivation) [8, 9]. Strikingly, analyses of the global gene expression profiles of *L. pneumophila* revealed that the pathogen's life cycle is very similar between *in vivo* infection models and *in vitro* broth cultures, as evidenced by the profound and comparable changes in gene expression during transition from the replicative phase (RP)/exponential growth phase to the transmissive phase (TP)/postexponential growth phase [10, 11]. Thus, the transition between the two phases, either within host cells or in cultures, is likely governed by a common virulence program engaged by *L. pneumophila* [10, 11].

The ability of *L. pneumophila* to survive and replicate depends on a well-balanced regulation of its biphasic life cycle [7, 8, 10, 12]. Previous proteomics and transcriptomics studies have demonstrated that the key metabolic pathways of

L. pneumophila are adapted to its biphasic life cycle (10, 11, 13, 14). For example, during the RP, genes related to metabolism, amino acid degradation, sugar assimilation, cell division, and biosynthetic processes are generally upregulated. In contrast, during the TP, genes associated with host entry, virulence, and survival, including those encoding Dot/Icm (defect in organelle trafficking/intracellular multiplication)-translocated effectors, motility machinery (flagellar and type IV pilus genes), enhanced entry proteins, and cyclic-di-GMP regulatory proteins, are upregulated. Hence, the transition between the RP and the TP requires a highly coordinated metabolic pathway (6). The biphasic life cycle is controlled by a multitude of regulatory elements that control gene expression, including regulatory proteins (*e.g.*, CsrA, RpoS, FliA, IHF), two-component systems (TCSs; *e.g.*, LetA/S, PmrA/B, LqsR/S), and stringent response metabolites (*e.g.*, RelA, SpoT, second messenger guanosine tetraphosphate (p) ppGpp) (12, 15–34). Therefore, the timely and fine-tuned expression of growth and virulence factors and adaptation traits in a life cycle–dependent manner is crucial. Several factors involved in the expression of virulence genes are also major regulators of metabolic pathways (15, 18), indicating that cellular differentiation and key metabolic changes play a significant role in the regulation of *L. pneumophila* virulence. However, the mechanisms underlying the regulation of these metabolic pathways and the function of multiple regulatory factors during this dimorphic life cycle are incompletely understood.

L. pneumophila virulence is characterized by the translocation of approximately 330 effector proteins into the host cells *via* the Dot/Icm type IVB secretion system (T4BSS), thereby triggering the recruitment of vesicles derived from the endoplasmic reticulum or the direct manipulation of various signaling pathways in the host cells (35–39). Notably, not all effectors are simultaneously translocated into the host cytosol at the onset of infection, suggesting that the temporal control of effector activity is required to effectively manipulate the host cell pathways (14, 40). Furthermore, the temporal control of some effectors in the host cell is consistent with their biological functions. For example, effectors SidM, LepB, and SidD target and antagonize Rab1 to temporally control its activation/deactivation on the *Legionella*-containing vacuole (LCV), whereas SidJ inhibits the ubiquitin ligase activity of the SidE family effectors (41–45). Since the translocation hierarchy of the effectors correlates with gene expression, the temporal control of effector activity may be achieved by regulating their expression levels (46). Several effectors, including the SidE family, SidC, and RalF, accumulate during the TP, suggesting that these function in very early infection when the bacteria are in contact with the host cell (47–49). Furthermore, proteomics revealed that a few effectors are exclusively synthesized during the RP and consequently will be secreted later than the TP effectors (14). However, the mechanisms underlying the regulation of life stage–specific effectors are still unknown.

Bacteria use regulated proteolysis for the degradation or activation of regulatory proteins to temporally control specific physiological processes and to mediate signaling pathways, such as stress response, growth, division, cell cycle, development with cell differentiation, pathogenesis, and protein secretion (50–55). Notable examples of temporal cell regulators include the competence regulator ComK in *Bacillus subtilis* and the stationary phase sigma factor RpoS in *Escherichia coli* and *Salmonella typhimurium* (56–58). We previously reported that the caseinolytic protease P (ClpP), the catalytic core of the Clp proteolytic complex that is conserved in most bacterial species, plays an integral role in the expression of transmission traits and regulation of life cycle transition and virulence of *L. pneumophila* (59–61). In our previous studies, we successfully constructed a strain with a *clpP* deletion (Δ*clpP*), using a nonpolar strategy without introducing any antibiotic resistance gene, in which the *clpP* gene alone was successfully knocked out, as validated by whole genome resequencing (59–61). Notably, our findings reveal that compared with the WT strain, the deletion of *clpP* delays the transition of *L. pneumophila* from the TP to the RP in liquid culture, impairs the survival and proliferation ability in host cells, and reduces the abundance of multiple effector proteins (59–61). Normally, ClpP is expressed throughout the life cycle of *Legionella*, indicating its essential role for protein hydrolysis (61). Although ClpP-dependent proteolysis was proven to be critical for *L. pneumophila*, the function of ClpP in regulating intracellular protein homeostasis and the role of regulatory proteins in life stage–specific expression are still unelucidated.

In this study, we aimed to investigate the dynamic profiles of global protein abundances during phase transition and to determine the function of ClpP in regulating the biphasic life cycle and pathogenesis of *L. pneumophila* using proteomic approaches. Such an integrative analysis has revealed the potential networks of interconnected proteins with substantial involvement in the life cycle transition of *L. pneumophila*. We further validated the requirement of ClpP-dependent proteolysis in regulating the abundance of the proteins for the regulation of *L. pneumophila* differentiation. Interestingly, we indicated that ClpP-dependent regulation of biphasic life cycle and bacterial virulence is independent. This study advances our understanding of *Legionella* in response to different conditions for replication and survival and provides additional evidence that the completion of the biphasic life cycle and bacterial pathogenesis is greatly dependent on protein homeostasis mediated by ClpP-dependent proteolysis.

EXPERIMENTAL PROCEDURES

Experimental Design and Statistical Rationale

To investigate the role of ClpP-mediated proteolysis in the regulation of life stage–specific proteins of *L. pneumophila*, the bacteria in the RP/TP of WT and Δ*clpP* were collected and analyzed by mass

spectrometry (MS). To screen the substrates of ClpP during the whole life cycle, bacterial whole-cell lysates from *clpP^wt* and *clpP^trap* in the TP were prepared and His-tagged proteins were purified with nickel–nitrilotriacetic acid affinity column (GE Healthcare) following the manufacturer's instructions. Substrates captured inside the proteolytic barrel were copurified along with the His-tagged ClpP complex and identified by MS to identify substrates of ClpP in the WT background. Each sample was analyzed in biological triplicates to allow for statistical tests and to improve consistency. Database searching of all LC–MS/MS raw files were analyzed with the Q Exactive HF-Orbitrap MS (Thermo Fisher Scientific, Co). Proteome Discoverer, version 2.2 software (Thermo Fisher Scientific, Co) was used for quality control and statistical processing. Only proteins identified in each of three biological replicates were quantified. Protein identification and quality criteria were very strict throughout the study with the label-free quantification. Protein abundances greater than 55 are considered significant (62). Student's *t* test ($p < 0.05$) was performed on the normalized protein intensities and defined as significant difference in protein abundance of two groups. Ratios of quantity of significantly different proteins were log2 transformed, and only those were approved who exceeded 1 or fell below −1 (14).

Bacterial Strains, Sample collection, Primers and Media

All *L. pneumophila* strains were cultured on buffered charcoal yeast extract (BCYE) plates, or in *N*-(2-acetamido)-2-aminoethanesulfonic acid–buffered yeast extract (AYE) medium, supplemented with thymidine (100 μg/ml) (63) when required. *E. coli* DH5α used as host strains for cloning strategies was grown in LB and agar at 37 °C. For liquid culture, AYE broth was inoculated with TP bacteria grown in the previous cycle to a final absorbance of 0.2 at 600 nm and incubated at 37 °C with vigorous shaking. RP bacteria were harvested at an absorbance of 0.7 to 1.0 at 600 nm, and TP bacteria were harvested approximately 6 h after the cessation of growth, which is at an approximate absorbance of 3.0 to 3.5 at 600 nm, according to the one previously reported (11, 61). *Acanthamoeba castellanii* (American Type Culture Collection 30234) was grown in proteose yeast extract glucose medium at 30 °C (64). To ascertain colony-forming units (CFU), serial dilutions of bacteria were incubated on BCYE for 4 days and resultant colonies were counted. The bacterial strains, plasmids, and primers used in this work are listed in supplemental Tables S18 and in S19 in the supplementary data, respectively.

Proteomic Analysis (LC–MS)

Proteomic analysis was performed as we previously described (61, 65). In brief, for each sample, 100 μg of protein was reduced with 10 mM DTT at 37 °C for 45 min, and iodoacetamide was then added to a final concentration of 15 mM, with incubation at room temperature for 1 h in the dark. The samples were then diluted with 100 mM ammonium bicarbonate buffer and digested with trypsin (1:50, trypsin/lysate ratio) for 16 h at 37 °C. Digests were centrifuged through 3 kDa filter tubes so that only digested peptides can go through. The concentrations of peptides were determined with a modified Lowry Protein Assay Kit (Sangon Biotech, Co). About 20 μg of peptides were desalted on Pierce C18 Spin Columns (Thermo Fisher Scientific, Co) according to the manufacturer's instructions.

Peptides were analyzed with the Q Exactive HF-Orbitrap MS. For each sample, the same amounts of peptides from total protein were separated on the analytical column with a 70 min linear gradient at a flow rate of 400 nl/min (0–3% B in 3 min; 3–8% B in 4 min; 8–32% B in 44 min; 32–99% B in 5 min; 99% B for 4 min; and 3% B for 10 min). The spectra were acquired in the positive ionization mode by data-dependent methods consisting of a full MS scan in high mass accuracy Fourier transform–MS mode at 60,000 resolution, with the precursor ion scan recorded over the *m/z* range of 350 to 1500.

Database searching of all LC–MS/MS raw files were done using Proteome Discoverer (version 2.2) against the UniProt *L. pneumophila* database (*L. pneumophila* subsp. pneumophila strain Philadelphia 1/American Type Culture Collection 33152/DSM 7513 proteome, last modified: October 26, 2018; 2930 proteins). For protein identification, the following options were used. Trypsin was specified as enzyme, cleaving after all lysine and arginine residues and allowing up to two missed cleavages. Carbamidomethylation of cysteine was specified as fixed modification. Protein N-terminal acetylation and oxidation of methionine were considered variable modifications. The peptide mass tolerance for precursor ions was set to 10 ppm, and the mass tolerance for fragment ions was set to 0.02 Da. "Maximum precursor mass" was set to 5000 Da, and "minimum precursor mass" was set to 350, and everything else was set to the default values, including the false discovery rate (FDR) limit of 5% on both the peptide and protein levels. The target with FDR <0.01 was defined as high confidence, and the target with 0.01 ≤ FDR <0.05 was defined as medium confidence. The threshold was based on a default FDR calculator using target/decoy strategy. Quantification abundances are normalized to the same total peptide amount per channel and scaled, so that the average abundance per protein and peptide is 100. Calculates quantification ratios for peptide-spectrum matches, peptides, and proteins based on precursor quantification. Details on identified proteins and peptides are provided in supplemental Tables S1 and S2, respectively.

In Vivo *Trapping of ClpP Substrate*

Proteomic analysis was performed as we previously described (61). The ClpP trapping system was constructed according to the previous report with minor modifications. Briefly, to generate the ClpP^trap, the active site (serine 110) of ClpP was replaced with an alanine (S110A). The plasmids expressing His-tagged ClpP^wt and ClpP^trap were transformed into Δ*clpP*, respectively, to create Δ*clpP*/p*clpP^wt* and Δ*clpP*/p*clpP^trap*. The Δ*clpP*/p*clpP^wt* and Δ*clpP*/p*clpP^trap* strains in TP were grown in 100 ml of AYE at 37 °C to an absorbance of 0.2 at 600 nm. To screen accumulated substrates of ClpP^trap during the whole life cycle, bacterial whole-cell lysates from Δ*clpP*/p*clpP^wt* and Δ*clpP*/p*clpP^trap* in the RP and TP were prepared, and His-tagged proteins were purified with nickel–nitrilotriacetic acid affinity column (GE Healthcare) following the manufacturer's instructions. Substrates captured inside the proteolytic barrel were copurified along with the His-tagged ClpP complex and identified by MS to identify substrates of ClpP in the WT background. Details on identified proteins and peptides are provided in supplemental Tables S3 and S4, respectively.

Data Analysis

Protein identification and label-free quantitation were performed with Proteome Discoverer, version 2.2 software using default setting. In the study, only proteins identified in each of three biological replicates were considered. Protein abundances greater than 55 are considered significant (62), and a Student's *t* test $p < 0.05$ was applied to identify proteins of two groups for which ratios of quantity of significantly different proteins were log2 transformed and only those were approved who exceeded 1 or fell below −1 (14). Functions of differential abundant proteins were queried from LegioList (http://genolist.pasteur.fr/LegioList/) and UniProt (https://www.uniprot.org/). Functional category annotation and gene essentiality were fetched from these websites. Voronoi treemaps have been proven as a powerful tool for the visualization of large proteomic data and functional relatedness of proteins in other research (14, 66–69). Thus, to visualize our complex dataset, we functionally mapped the quantified *L. pneumophila* proteome based on their annotation and prediction.

Kyoto Encyclopedia of Genes and Genomes (KEGG) enrichment analysis was performed using the OmicShare tools, a free online

platform for data analysis (http://www.omicshare.com/tools), which significantly enriched pathways were retrieved by searching against KEGG databases. Protein–protein interaction network construction was performed using STRING web service (https://string-db.org/) (a database of known and predicted protein–protein interactions) with the differentially expressed proteins revealed by proteomic data used as input. The integrated network analysis results based on a required minimum interaction score of at least 0.7 by STRING database were output by Cytoscape software (https://cytoscape.org/), version 3.7.2. Random forest analysis to investigate the contribution of the putative proteins to the biphasic life cycle transition (70). Analyses were conducted in RStudio (RStudio, PBC), version 3.5.0, to produce heatmaps and random forest analysis (71).

Construction of the Ectopic Expression Plasmids

The ectopic expression strains were performed as we previously described with minor modifications (61). Briefly, the sequences of *lpg0361*, *lpg0362*, *lpg0102*, and *spoT* gene were amplified by PCR using the primer pairs P*lpg0361*-F/P*lpg0361*-R, P*lpg0362*-F/P*lpg0362*-R, P*lpg0102*-F/P*lpg0102*-R, and P*spoT*-F/P*spoT*-R, respectively. The PCR products were digested with BamHI and XhoI and subcloned into the ectopic plasmid pJB908, creating plasmid pJB908-*lpg0361*, pJB908-*lpg0362*, pJB908-*lpg0102*, and pJB908-*spoT*. A hexahistidine tag was added to the C terminus of the protein in all the resulting recombinant plasmids pJB908-*lpg0361*, pJB908-*lpg0362*, pJB908-*lpg0102*, and pJB908-*spoT* during cloning. The resultant plasmid pJB908-*lpg0361*, pJB908-*lpg0362*, pJB908-*lpg0102*, and pJB908-*spoT* was electroporated into WT and Δ*clpP* to create ectopic strain WT/p*lpg0102*, WT/p*lpg0361*, WT/p*lpg0362*, WT/p*lpgspoT*, Δ*clpP*/p*lpg0102*, Δ*clpP*/p*lpg0361*, Δ*clpP*/p*lpg0362*, and Δ*clpP*/p*spoT*, respectively.

Growth Curve Assay

Growth curve assay was performed as we previously described (61). Fresh *L. pneumophila* cells were inoculated into 5 ml of AYE(T) medium and were cultured to the TP at 37 °C. Then the cultures were transferred into 50 ml of AYE in flasks, incubated to the TP, then diluted into new flasks to similar absorbances at approximate absorbance of 0.2 at 600 nm at time 0. Cultures were grown at 37 °C with shaking. To measure the growth curve, 1 ml of the cells was sampled every 3 h for measurement of absorbance at 600 nm. To ensure conformity, multiple replicates on different days were examined. All experiments were performed in biological triplicate.

RNA Isolation, Complementary DNA Preparation, and Quantitative RT–PCR

Quantitative RT–PCR (qRT–PCR) was performed as we previously described (61). RNA for real-time qRT–PCR was prepared using an Eastep Super Kit following manufacturer's protocols (Promega Co) and treated with DNase I according to the manufacturer's instructions (Promega Co) prior to complementary DNA preparation. Complementary DNA was prepared using GoScript Reverse Transcription System as described by the manufacturer (Promega Co). qRT–PCR was performed in a 20 μl reaction volume using an Applied Biosystems StepOne Plus 96-well RT–PCR system with Power SYBR Green PCR Master Mix following the manufacturer's instructions (Applied Biosystems Co). 16S rRNA was used as the reference sample in all comparative threshold cycle (ΔΔCT) experiments. All qRT–PCR primers were tested for amplification efficiency. qRT–PCR data were analyzed using StepOne System software (Applied Biosystems, Inc) and GraphPad Prism (GraphPad Software, Inc). Primers used in qRT–PCR experiments are shown in supplemental Table S19. All analyses were performed in biological triplicate.

Bacterial Infectivity in A. castellanii

Bacterial infectivity and intracellular growth were performed as we previously described (61). The *A. castellanii* cells were seeded onto a 24-well plate (5×10^5 per well) allowing to adhere for 2 h prior infection. *L. pneumophila* cells were grown for 20 h in AYE broth at 37 °C with shaking, diluted in HL5, and were used to infect amoebae at a multiplicity of infection of 10. About 30 min postinfection, extracellular bacteria were removed by washing three times with warm HL5 medium (21). At each time points indicated, culture supernatant was removed, and the amoebae cells were lysed with 0.04% Triton. The supernatant and lysates were combined, and serial dilutions were prepared and aliquots were plated on BCYE plates for CFU counting (72). All experiments were performed in triplicate at 30 °C.

Protein Isolation and Western Blot

Protein isolation and Western blot were performed as we previously described (61). Total cell extracts of *L. pneumophila* were prepared at various time points after growth at 37 °C. Briefly, bacterial cell pellets were resuspended in 1 ml of lysis buffer and sonicated for 2 min. The cells were then centrifuged for 1 h at 120,00*g*. The protein-containing supernatant was removed, and the protein concentration was measured using a commercial kit (Bio-Rad Co). Samples were normalized for protein loading and run on a 10% SDS-PAGE as described previously (73). Western blot was carried out as described elsewhere (74). The levels of Lpg0102, Lpg0361, Lpg0362, or SpoT were immunoblotted with anti-His tag antibody. Isocitrate dehydrogenase was probed as a loading control.

RESULTS

Growth Phase–Dependent Protein Expression Profiles of *L. pneumophila*

To investigate the significance of ClpP-dependent proteolysis in regulating the biphasic life cycle and virulence of *L. pneumophila* (Fig. 1*A*), we performed a proteomic analysis of whole lysates obtained from cultures of *L. pneumophila* WT at the RP and TP to acquire a comprehensive proteomic profile of the two phases and to identify the proteins that are differentially expressed per life stage (Fig. 1*B*). A total of 1927 differentially expressed proteins between the RP and TP were identified and quantified (Table 1). These proteins represent 65.48% of the annotated proteins, consisting of 2943 open reading frames, in *L. pneumophila* Philadelphia-1 proteome (75). The expression levels of 428 proteins (22.21%) showed significant differences between the RP and TP (supplemental Tables S5 and S6), including 220 and 208 proteins that were upregulated in the RP (RP-on and RP-up) and TP (TP-on and TP-up), respectively, which were above or below the threshold of +1 and −1 log2(RP/TP) (supplemental Fig. S1*A*). Both groups contained a number of on/off proteins solely identified either in the RP or in the TP, including 23 that were RP-on (synonymously TP-off) and 11 that were TP-on (synonymously RP-off).

The KEGG pathway enrichment analysis was subsequently performed to functionally annotate differentially expressed proteins between the RP and TP. We discovered that during the RP, the proteins associated with the pathways for ribosome, amino sugar, nucleotide sugar metabolism, and biotin
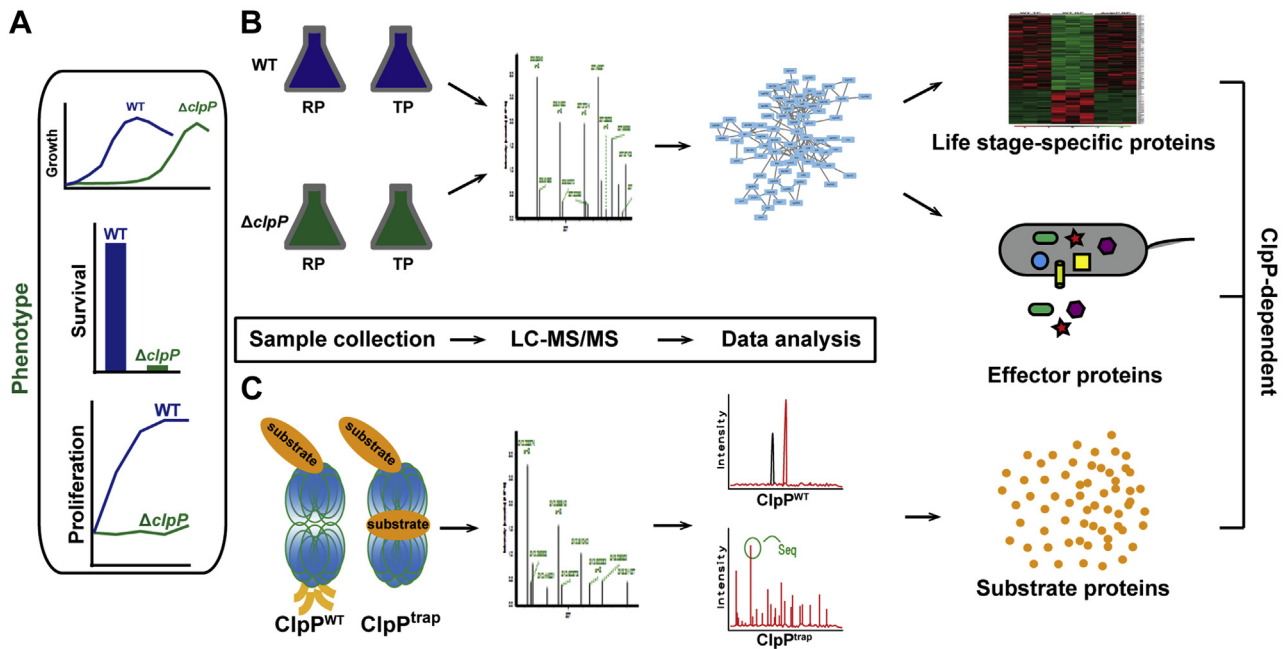
FIG. 1. **Schematic representation of the proteomic study of ClpP-dependent proteolysis in *Legionella pneumophila*.** *A*, our previous findings showed that deletion of *clpP* delays the entry of the replicative phase (RP) of *L. pneumophila* in liquid culture and impairs survival and the proliferation ability in host cells (59–61). *B*, schematic visualization of the whole proteome analysis in WT and Δ*clpP* strain at the RP and the transmissive phase (TP). For liquid culture, AYE broth was inoculated with TP bacteria grown in the previous cycle to a final absorbance of 0.2 at 600 nm and incubated at 37 °C with vigorous shaking. RP bacteria were harvested at an absorbance 0.7 to 1.0 at 600 nm, and TP bacteria were harvested approximately 6 h after the cessation of growth, which is at an approximate absorbance of 3.0 to 3.5 at 600 nm. *C*, *in vivo* trapping of ClpP substrate proteins. Substrates captured inside the proteolytic barrel were copurified along with the His-tagged ClpP complex and identified by mass spectrometry to identify substrates of ClpP in the WT background. AYE, *N*-(2-acetamido)-2-aminoethanesulfonic acid–buffered yeast extract; ClpP, caseinolytic protease P.

metabolism were the most significantly enriched, followed by those related to the pathways for homologous recombination, base excision repair, fatty acid biosynthesis, and mismatch repair (supplemental Fig. S1*B*). The RP-specific proteins were found to play vegetative functions for growth and reproduction (*e.g.*, RplS, RpsH, RpsP, RpmA, RpsT) and cell division (*e.g.*, FtsA, FtsQ, FtsZ) (supplemental Fig. S1*C*). Overall, the RP-specific pathways are mainly responsible for bacterial replication and growth. In contrast, TP-specific proteins were related to multiple microbial metabolic pathways, such as propanoate metabolism and synthesis and degradation of

ketone bodies. Poly-3-hydroxybutyrate, the main carbon and energy storage for *L. pneumophila* that is utilized under nutrient starvation conditions (13, 76–78), was promoted by PhaB (acetoacetyl-CoA reductase), AcsB (acetyl-CoA synthetase), AtoB (acetyl-CoA C-acetyltransferase), and BdhA (3-hydroxybutyrate dehydrogenase) (supplemental Fig. S1*D*). As previously suggested (7, 8, 12), we also confirmed that majority of the flagellar assembly proteins (*e.g.*, MotA, FlgH, FlgI, FlgA, FlhF, Lpg0907, FliA, FliS, PilM), signal transduction proteins (*e.g.*, LetE, YhbH, PilR, YegE, Lpg0829, RpoS, LqsR), and oxidoreductase-related proteins (*e.g.*, MmsA, PntB,

TABLE 1
Overview of identified protein of L. pneumophila *RP and TP in the WT and ΔclpP strain, respectively*

∑Ident	Fraction		RP		TP		∑Ident	Percentage[a] (%)
			RP-On	RP-Up	TP-On	TP-Up		
1927	WT	Life cycle	23	197	11	197	428	14.54
	Δ*clpP*[b]	Up					(316) 629	(73.83) 21.37
		Down	(156) 255		(111) 152			
			(68) 198		(40) 128			

[a]Percentage of total different proteins found compared with 2943 ORFs corresponding to the *L. pneumophila* Philadelphia-1 genome (GeneBank accession: AE017354.1).
[b]The numerical value in parentheses means the numbers of protein that were RP or TP specific in the WT.

TABLE 2
Summary of ClpP-regulated proteins identified by LC–MS during the biphasic life cycle

No.	Pathways/functional category	Number of proteins	
		RP	TP
1	Virulence effector	93	52
2	Dot/Icm apparatus	6	4
3	Toxin production, other pathogen functions	7	6
4	Flagellar assembly, motility	10	9
5	Transcription, RNA stability; translation	32	22
6	Regulation; two component system; signal transduction	26	17
7	Cell envelope, cell division	10	15
8	Glycan biosynthesis and metabolism	3	7
9	Protein secretion/trafficking, protein fate	30	16
10	Nucleotide metabolism	13	5
11	DNA replication, recombination and repair	7	11
12	Aminoacid metabolism, other aminoacids	34	16
13	Fatty acid/lipid metabolism	12	4
14	Carbohydrate metabolism and energy	32	21
15	Cofactors and vitamins, secondary metabolite	32	26
16	Transport, uptake	23	13
17	Stress response, defence; xenobiotica	17	6
18	Unknown, hypothetical proteins; others	117	63

MaeA) were upregulated in the TP. Collectively, the TP specific primarily facilitates the expression of transmissive traits.

These results provide more detail data for understanding the mechanism of how *L. pneumophila* adopted a reciprocal biphasic life cycle and revealing an unexpected complex picture of life cycle–dependent regulation profiles of *L. pneumophila*.

ClpP-Dependent Proteolysis Plays an Important Role in Maintaining the Biphasic Life Cycle

To adapt to the biphasic life cycle, *L. pneumophila* employs a bipartite metabolism that requires fine-tuned regulation (6, 7, 77). Since our previous study revealed that ClpP is necessary for the transition from the TP to RP (Fig. 1*A*), we then used the Δ*clpP* strain to investigate the differences in ClpP-dependent regulatory proteins at the RP and TP on a large scale (Fig. 1*B*). To avoid the unknown affection of extra plasmid (and the antibiotic resistance gene) on the physiology of *Legionella* and facilitate the carried out experiments, the whole genomes of WT and Δ*clpP* have been resequenced and compared. It showed that only the *clpP* gene alone was successfully knocked out in Δ*clpP* strain (supplemental Fig. S2). Compared with the WT, a total of 629 proteins showed significantly different levels in the Δ*clpP* strain, corresponding to 32.64% of the identified proteins (*i.e.*, 21.37% of the annotated proteins in the *L. pneumophila* Philadelphia-1 proteome) (Table 1). These included 453 proteins with different abundances at the RP (255 were upregulated and 198 were downregulated) and 280 proteins with different levels at the TP (152 were upregulated and 128 were downregulated) (supplemental Tables S7–S10). Furthermore, Voronoi treemaps were used to comprehensively characterize the proteomic data at the RP

and TP between the Δ*clpP* strain and WT as well as determine the role of ClpP during the transition between phases (14, 66–69). The red and green fonts indicate that the protein levels were upregulated and downregulated, respectively, in the Δ*clpP* strain compared with the WT at the RP or the TP (Table 2 and Fig. 2).

Based on the Voronoi treemaps, the downregulated proteins in the RP of the Δ*clpP* strain were found to be related to the functional categories for "DNA replication, recombination and repair," "Transport, uptake," "Dot/Icm apparatus," "Cell envelope, cell division," and "Glycan biosynthesis and metabolism," whereas the upregulated proteins in the RP were related to the functional categories for "Carbohydrate-metabolism and energy," "Stress response, defense, xenobiotics," "Amino acid metabolism, other amino acids," "Flagellar assembly, motility," "Regulation, TCS, signal transduction," and "Nucleotide metabolism" (Figs. 2, S3 and supplemental Table S11). Interestingly, the upregulated proteins in the RP of the Δ*clpP* strain were greatly enriched in the pathways for TCSs, microbial metabolism, and flagellar assembly, which were previously observed in the TP of the WT (supplemental Fig. S4*A*). In addition, the downregulated proteins in the RP of the Δ*clpP* strain were greatly enriched in the pathways for biotin metabolism, fatty acid metabolism, ABC transporters, and ribosomes, which were previously observed in the RP of the WT (supplemental Fig. S4*B*). The discrepancies in the metabolic pathways observed during the RP in the Δ*clpP* strain suggest that ClpP-dependent proteolysis is essential for the normal function of RP-specific proteins. Moreover, the interaction network analysis showed that the upregulated proteins in the RP of Δ*clpP* strain were associated with flagellar assembly (*e.g.*, FliS, Lpg0907, FlgD, FlgE, FliA, FlgI,
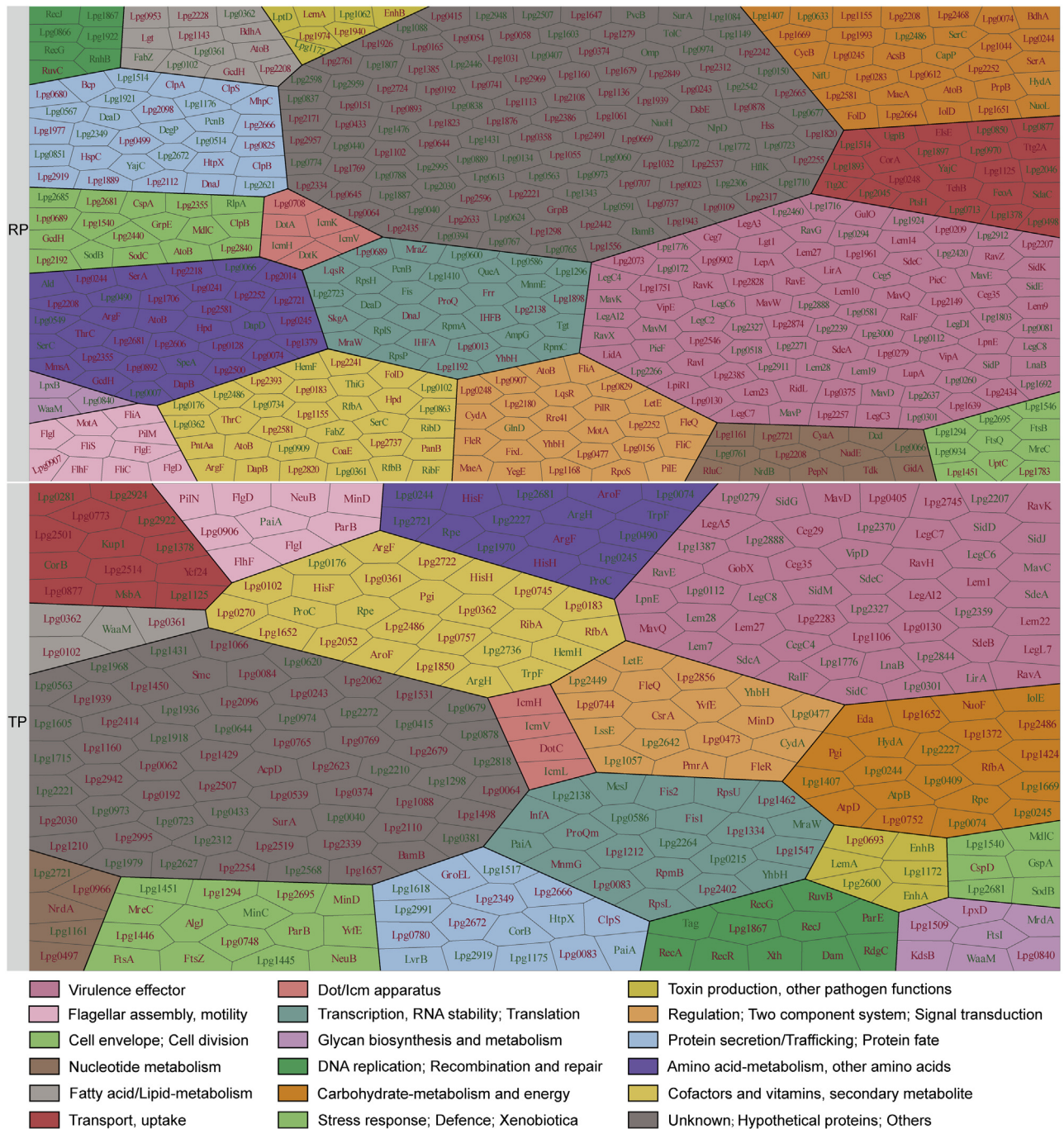
FIG. 2. Quantity of ClpP-regulated proteins according to functional relatedness in the replicative phase (RP) and the transmissive phase (TP) of *Legionella pneumophila*. The Voronoi treemap visualizes functionally organized quantitative information as area of hierarchically organized information on abundance of proteins at either RP or TP in the ΔclpP strain compared with WT strain. Proteins were clustered according to their functional categories as areas of different colored mosaic tiles, and the ratios of protein abundance in the RP/TP were highlighted in the treemaps. *Red font* indicates the protein levels that are upregulated at the RP or the TP in ΔclpP strain compared with WT strain (supplemental Tables S7 and S9), *green font* indicates the protein levels that are downregulated in the RP or the TP in ΔclpP strain compared with WT strain (supplemental Tables S8 and S10). Proteins were clustered according to their functional categories as areas of different colored mosaic tiles (supplemental Tables S11 and S12). The protein functions represented by different colors are noted below the figure. ClpP, caseinolytic protease P.

MotA, FliC, FlhF, Lpg1783, PilM), signal transduction (*e.g.*, YegE, Rre41, Lpg0156, Lpf1490, Lpg0829, Lpg2180, LqsR, RpoS, Lpg0477, PilR, FixL), transcriptional regulators (*e.g.*, FleQ, FleR, MraZ, SkgA, IHFA, IHFB), ATP-binding protease components (*e.g.*, ClpA, GrpE, DnaJ, ClpB, ClpS), and microbial metabolism in diverse environments (*e.g.*, Lpg2664, Lpg0245, AcsB, AtoB) (supplemental Fig. S4*C*). In addition, the downregulated proteins in the RP of the Δ*clpP* strain were found to interact with ribosomal proteins (*e.g.*, RplS, RpsH, RpmC, RpsP, RpmA), cell division proteins (*e.g.*, Lpg0934, PilF, Lpg0394, FtsB, FtsQ), lipid metabolism proteins (*e.g.*, FabZ, Lpg0102, Lpg0361, Lpg0362), and outer membrane proteins (*e.g.*, OstA, SurA, BamB, Lpg0840, LpxB) (supplemental Fig. S4*D*). These results suggest that the fine-tuned regulation of these proteins is important during the RP.

Moreover, in the TP of the Δ*clpP* strain, the downregulated proteins were primarily under the functional categories for "Amino acid metabolism, other amino acids," "Stress response, defense, xenobiotics," and "Toxin production, other pathogen functions," whereas the upregulated proteins were under the functional categories for "Flagellar assembly, motility," "Cofactors and vitamins, secondary metabolite," "Fatty acid/lipid metabolism," "DNA replication, recombination and repair," "Cell envelope, cell division," and "Transcription, RNA stability, translation" (Figs. 2, S3 and supplemental Table S12). The KEGG pathway analysis revealed that the upregulated proteins in the TP of the Δ*clpP* strain were highly enriched in the pathways for amino sugar and nucleotide sugar metabolism, homologous recombination, biotin metabolism, fatty acid metabolism, and base excision repair, which were previously observed for the RP-specific proteins in the WT (supplemental Fig. S5*A*). Furthermore, the downregulated proteins in the TP of the Δ*clpP* strain were greatly enriched in the pathways for microbial metabolism, and TCSs, which were previously observed for the TP-specific proteins in the WT (supplemental Fig. S5*B*). These results suggest that the functional loss of ClpP could cause a disorder in the metabolic pathways involved by the TP-specific proteins, confirming that ClpP-dependent proteolysis is also essential during the TP. In addition, the interaction network analysis demonstrated that the upregulated proteins in the TP of the Δ*clpP* strain were associated with ribosomal proteins (*e.g.*, RpsL, RpmB, RpsU), cell division proteins (*e.g.*, ParB, Lpg1446, FtsA, FtsZ), cell envelope synthesis (*e.g.*, Lpg0840, Lpg0768, Lpg0748, YvfE), flagellar assembly (*e.g.*, Lpg0906, FlgI, FlgD, FlhF, FleQ), and lipid metabolism (*e.g.*, LipA, Lpg0102, Lpg0361, Lpg0362) (supplemental Fig. S5*C*), whereas the downregulated proteins in the TP of the Δ*clpP* strain were related to signal transduction (*e.g.*, sensory box GGDEF family proteins LssE, Lpg2642), pathogen function (*e.g.*, IcmL, EnhB, EnhA, LemA), and crosslinking of the peptidoglycan cell wall (*e.g.*, MrdA, FtsA) (supplemental Fig. S5*D*). In the proteome data, we found that Lpg0279, a TCS regulator expressed at the TP and promotes both *L. pneumophila* cell differentiation and survival

(79), was decreased during the TP in the absence of *clpP*, compared with WT. Moreover, the low expression of protein NrdA or LipA was required during the TP (no significant difference in the RP) in the WT, but a high expression level was detected in the TP of the Δ*clpP* strain. Also, the accumulation of NrdA or LipA during the TP caused a prolonged lag phase from the TP to the RP of *L. pneumophila* (supplemental Fig. S6). These results suggest that the temporal regulation of these proteins may be vital during the TP.

Because of the complexity of the ClpP-mediated network, specific regulatory proteins and predictable effects of their respective changes were also observed in the proteome. As shown in supplemental Fig. S7, compared with that CsrA was highly accumulated in the Δ*clpP* mutant than in WT during the TP, the expression of LetE and CegC4 was significantly decreased in the Δ*clpP* strain than in the WT, whereas the expression of Lem27 was significantly increased in the Δ*clpP* strain than in the WT (supplemental Fig. S7, *A–D*). The Δ*clpP*/ p*csrA* strain was used to further investigate whether the effect of these proteins was related to CsrA. Compared with that in the Δ*clpP*/p*csrA* and Δ*clpP*/pJB908, the expression of *csrA* was significantly increased, and correspondingly, the expression of *letE* and *cegC4* was indeed downregulated and the expression of *lem27* observed was indeed upregulated (supplemental Fig. S7, *E–H*). These data were in consistent with the study by Sahr *et al.* (18).

Taken together, comparison of the bipartite metabolic proteins between the WT and Δ*clpP* strain using Voronoi treemaps, KEGG pathway enrichment, and interaction network analysis revealed that the regulation of the regulatory proteins *via* ClpP-dependent proteolysis is crucial in maintaining the biphasic life cycle of *L. pneumophila*.

ClpP Controls the Biphasic Life Cycle–Dependent Protein Turnover Between the RP and the TP

To further explore the function of ClpP-dependent proteolysis in regulating the transition of the biphasic life cycle, we analyzed the abundance of 428 RP- and TP-specific proteins between the Δ*clpP* strain and WT (supplemental Table S13). A total of 316 life stage–specific proteins (73.83%) were observed that their growth-dependent expression was linked to the regulation of ClpP-dependent proteolysis (Table 1). Notably, the Voronoi treemap demonstrated that most of the proteins were regulated *via* ClpP, including proteins that were classified under the following functional categories: "Regulation, TCS, signal transduction," "Dot/Icm apparatus," "Toxin production, other pathogen functions," and "Cell envelope, cell division." The remaining proteins belonged to the following categories: "Virulence effector," "Carbohydrate metabolism and energy," "Fatty acid/lipid metabolism," "Amino acid metabolism, other amino acids," "Stress response, defense, xenobiotic," "Protein secretion/trafficking, protein fate," "Nucleotide metabolism," "DNA replication, recombination, and repair," "Cofactors and vitamins,

secondary metabolite," and "Flagellar assembly, motility" (Figs. 3 and S8). These data indicate the significant contribution of ClpP-dependent proteolysis in the timely regulation of protein expression levels at different phases.

Transcriptional control is crucial for the regulation of *L. pneumophila* differentiation to activate the genes necessary for adapting to new conditions and to repress the genes that are no longer required (30). In this study, we discovered that the abundance of key transcriptional regulators was controlled in a ClpP-dependent manner (supplemental Table S14). The downregulation of several RP-specific regulators in the TP of WT depended on ClpP, including Fis1, Fis2, and Fis3 (regulators that repress the expression of numerous effector-encoding genes) (80) and Lpg1212 (a MarR transcriptional regulatory protein) (81–84). Notably, several TP-specific proteins that were downregulated in the RP of the WT were upregulated in the ΔclpP strain, including Lpg0689 (a Dps-like DNA-binding stress protein previously found abundant in starved *E. coli* that can be DNase resistant when complexed with DNA) (85–87), Lpg1192 (a ThiJ/PfpI family transcriptional regulator) (88), DnaJ (a curved DNA-binding protein) (89–92), MraZ (a DNA-binding transcription factor; its overproduction in *E. coli* inhibited cell division) (93), LqsR (a novel pleiotropic regulator involved in regulating the bacterial growth phase switch, pathogen–host cell interactions, motility, natural competence, and filament production) (21, 94–96), and IHFA/IHFB (two integrating host factors that form a heterodimer and

play an integral role in the global regulatory system governing the transition from the RP to TP) (26, 27). In addition, the TP-specific proteins, Lpg2138 (a transcriptional regulator that regulates a diverse set of genes involved in virulence, metabolism, quorum sensing, and motility) (81, 97, 98) and YhbH (a hibernation-promoting factor that is expressed during the stationary phase) (99, 100), were less abundant in the RP of the WT (*i.e.*, more abundant in the TP of the WT), but become more abundant in the RP and less abundant in the TP, in the absence of *clpP*. These results indicate that the alteration in the abundance of ClpP-dependent transcriptional regulators at different stages is essential for normal function at a specific phase in the life cycle of *L. pneumophila*.

Like other bacterial pathogens, *L. pneumophila* employs a variety of distinct TCSs to control post-transcriptional regulation (6, 101) and govern the differentiation between the RP and the TP (21, 79, 102–105). Here, we confirmed that the regulation of several TCS proteins and proteins under the control of TCSs was ClpP dependent (supplemental Table S15). In the absence of *clpP*, several TP-specific TCSs were observed to be upregulated at the RP, including Lpg0829 (a LapD-like c-di-GMP receptor that can act as a coincidence detector) (106, 107), PilR (a sigma 54 activator protein that interacts with RpoN for transcription initiation) (108), and LqsR (a two-component response regulator that also acts as a transcriptional regulator) (21, 94–96). Notably, the RP-specific protein PmrA (directly interacts with the
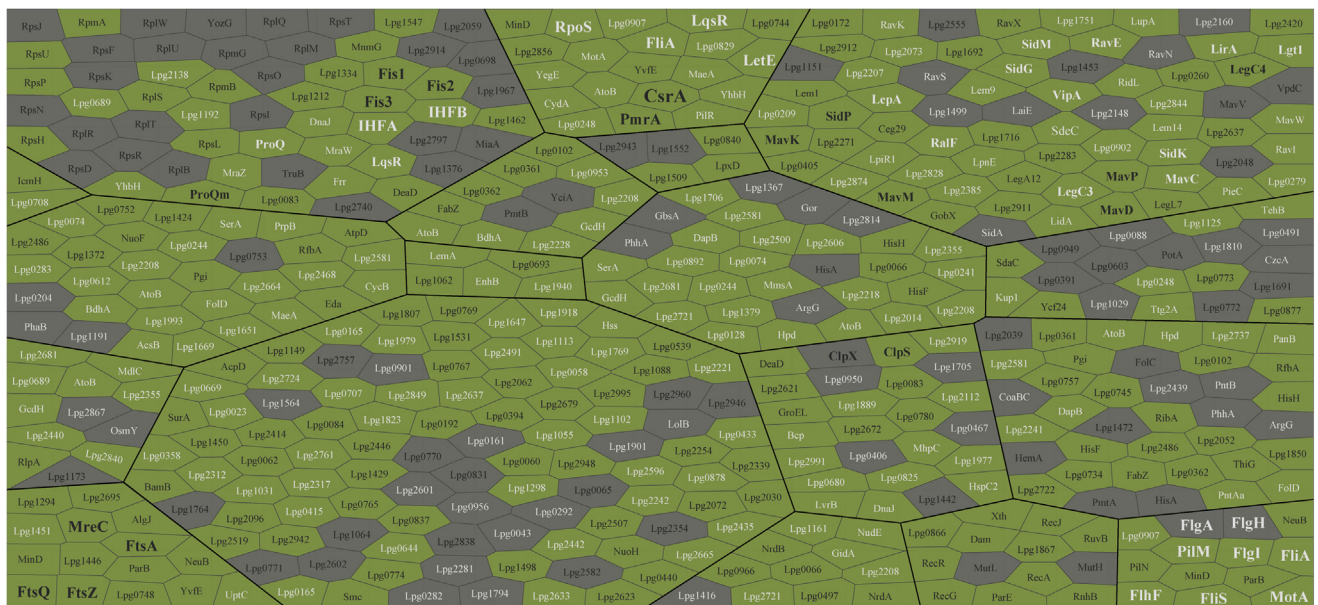

FIG. 3. **A treemap showed 428 of life cycle–dependent proteins, which are regulated or not regulated by ClpP.** The Voronoi treemap visualizes hierarchically organized information of 428 of life cycle–dependent proteins (supplemental Table S13). *Black font* indicates that the protein is expressed highly at the replicative phase (RP) in the WT strain, and *white font* indicates that the protein is expressed highly at the transmissive phase (TP) in the WT strain. Proteins were clustered according to their functional categories as area of different color mosaic tiles. *Green polygons* indicate that the protein levels are regulated by ClpP, and *gray polygons* indicate that the protein levels are not regulated by ClpP. The proteins in *bold font* indicate that they have been known to be important to the life cycle and virulence of *Legionella pneumophila*. ClpP, caseinolytic protease P.

sensor kinase PmrB; it not only activates the expression of 43 effector-encoding genes but also positively regulates CsrA (24, 104)) was downregulated in the TP of the WT but upregulated in the Δ*clpP* strain. In addition, several TP-specific proteins involved with TCSs that were less abundant in the RP of the WT had a higher level in the Δ*clpP* strain, such as CydA (cytochrome D ubiquinol oxidase subunit I; plays an important role in cell growth and stress resistance in *E. coli* (109, 110)) and FliA (an RNA polymerase sigma factor involved in the regulation of flagellum production; also acts as a regulator of virulence genes that are required for the expression of pathways for cytotoxicity, lysosome evasion, and replication in *L. pneumophila* (111–113)). In addition, the RNA polymerase sigma factor RpoS (involved in the regulation of multiple pathways associated with motility and pathogenic functions as well as the activity of transcriptional regulators and Dot/Icm effectors) (19, 20, 22) observed at the RP had a lower level in the WT than in the Δ*clpP* strain. The transmission trait enhancer LetE (a connector protein between the CpxRA TCS and the LetAS-RsmYZ-CsrA regulatory cascade) (114) was less abundant at the RP in the WT (*i.e.*, more abundant at the TP in the WT) but become more abundant at the RP and less abundant at the TP in the Δ*clpP* strain. Similarly, the RP-specific global regulator CsrA (a pivotal repressor of transmission traits and activator of replication) (12) that was less abundant in the TP of the WT had a higher level in the Δ*clpP* strain.

To systematically determine the role of ClpP in regulating the life stage–specific proteins, we subsequently analyzed the dynamic changes of phase-specific 316 proteins during the transition from the TP to the RP and vice versa (Fig. 3). During the TP to RP transition, ClpP-dependent proteolysis was confirmed to be essential for downregulating 154 TP-specific proteins and upregulating 68 RP-specific proteins (supplemental Fig. S9, *A* and *B*). The TP-specific proteins were observed to be highly enriched in 13 significant pathways (*e.g.*, microbial metabolism, TCSs, flagellar assembly), whereas the RP-specific proteins were mainly enriched in the pathways for biotin metabolism, fatty acid biosynthesis, fatty acid metabolism, base excision repair, and ribosome metabolism (supplemental Fig. S9*C*). The integrated network analysis showed that the key proteins involved in the TP to RP transition, including Lpg2664, AcsB, MmsA, AtoB, FliA, FliS, FlhF, Frr, Lpg0358, and Lpg2228, presented decreased abundance, whereas Lpg0102, Lpg0361, Lpg0362, FabZ, RpmA, RplS, RpsP, RpsH, Lpg0394, and FtsQ increased in abundance (supplemental Fig. S9*D*). During the RP to TP transition, ClpP-dependent proteolysis caused the downregulation of 108 RP-specific proteins and the upregulation of 40 TP-specific proteins (supplemental Fig. S10, *A* and *B*). Furthermore, the RP-specific proteins were found to be highly enriched in the pathways for amino sugar and nucleotide sugar metabolism, homologous recombination, fructose and mannose metabolism, and biotin metabolism, whereas

TP-specific proteins were mainly enriched in the pathways for degradation of aromatic compounds, aminobenzoate degradation, starch and sucrose metabolism, and benzoate degradation (supplemental Fig. S10*C*). The integrated network analysis also revealed that the key proteins involved in the RP to TP transition, including RecA, LipA, Lpg0361, Lpg0362, Lpg0102, RfbA, Lpg2486, Pgi, Lpg0757, YvfE, Lpg0906, HisF, HisH, NeuB, Lpg0748, Lpg0768, and Lpg0769, presented decreased abundance, whereas Lpg0420 increased in abundance (supplemental Fig. S10*D*).

Taken together, these results suggest that *L. pneumophila* employ ClpP-dependent proteolysis to either degrade or activate regulatory proteins and control their expression at a specific life stage, leading to the temporal and spatial regulation of the processes required for morphological development. The reciprocal regulation of the RP and TP mediated by ClpP may aid in the successful adaptation of *Legionella* to harsh environments.

Fatty Acid Biosynthesis–Related Proteins Play an Important Role During Phase Transition

The strict regulation of differentiation is critical for the biphasic life cycle of *L. pneumophila* (6, 7). Thus, we also investigated whether the levels of selected life stage–specific proteins were regulated in a ClpP-dependent manner during both phases. Fifty-nine proteins (13.79%) were successfully screened and quantified (Figs. 4, S11 and supplemental Table S16), indicating their significant functions during both the RP and TP. The Voronoi treemaps showed that at either phases, the levels of the identified proteins in the WT were influenced by ClpP. Three proteins, namely Lpg0102, Lpg0361, and Lpg0362, were found to be under the "Cofactors and vitamins, secondary metabolite" and "Fatty acid/lipid metabolism" categories. These proteins also showed the highest confidence (0.900) among the interactions after the STRING web service analysis.

Since the ClpP deletion delayed the TP to RP transition ((61), Fig. 1*A*), we postulated that the identified differentially expressed proteins may be critical during this process. The KEGG pathway analysis revealed that the 59 life stage–specific proteins were significantly enriched in the pathways for biotin metabolism, fatty acid biosynthesis, and fatty acid metabolism (supplemental Fig. S12*A*). Notably, Lpg0102 (3-oxoacyl-acyl carrier protein [ACP] synthase) (FabF), Lpg0361 (3-oxoacyl-ACP synthase 2) (FabB), and Lpg0362 (FabB, N-terminal region) were also highly enriched (supplemental Fig. S12*B*). Random forest analysis (70) further revealed that 30 of the identified proteins potentially perform a significant role in mediating the transition process (supplemental Fig. S12*C*), including Lpg0361, Lpg0362, and Lpg0102. Collectively, these results suggest that specific fatty acid biosynthesis–related proteins may have essential functions during phase transition.
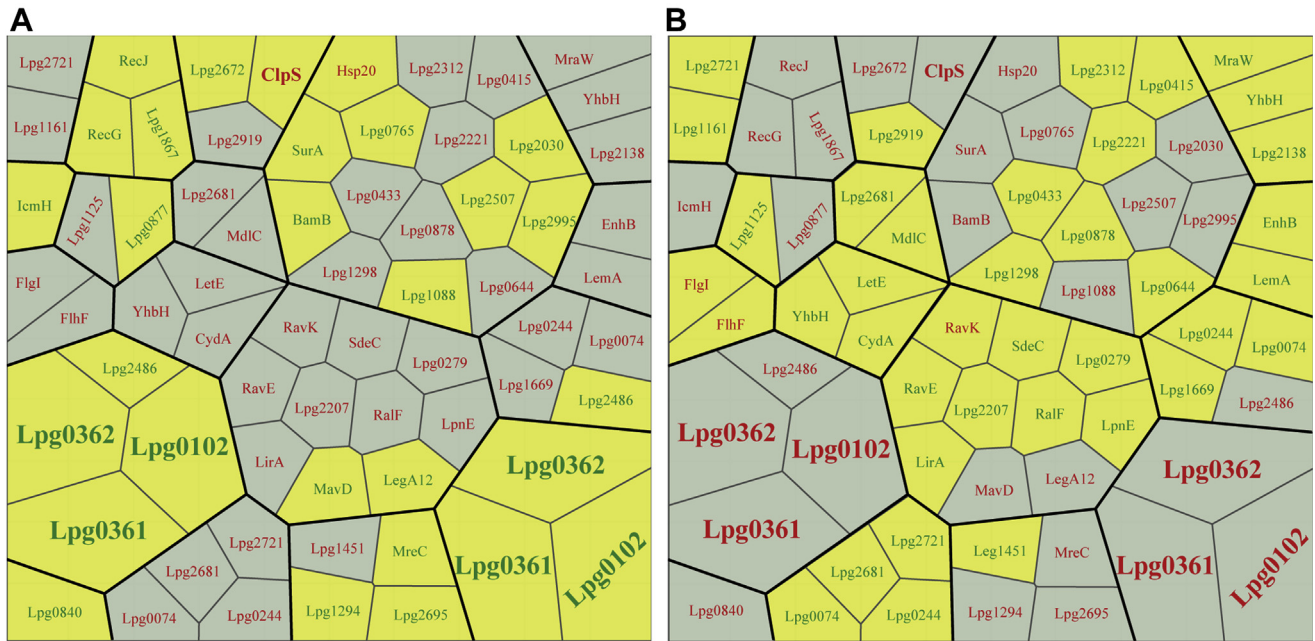
FIG. 4. **The Voronoi treemap visualizes 59 growth stage–specific proteins regulated by ClpP both at the replicative phase (RP) and the transmissive phase (TP).** The Voronoi treemap visualizes hierarchically organized information of 59 life cycle–dependent proteins during the RP (*A*) and the TP (*B*) (supplemental Table S16). Proteins were clustered according to their functional categories. *Yellow polygons* indicate the proteins with higher expression at the indicated phase in the WT, and the *green fonts* indicate that the protein level is decreased in Δ*clpP* strain. *Gray polygons* indicate the proteins with lower expression at the indicated phase in the WT, and the *red fonts* indicate that the protein level is increased in Δ*clpP* strain. Proteins were manually adjusted to *bold font* according to a highest confidence (0.900) in the interaction among them. ClpP, caseinolytic protease P.

Lpg0102, Lpg0361, and Lpg0362 Protein Levels are Critical for Phase Transition

To explore the function of fatty acid biosynthesis–related proteins Lpg0102, Lpg0361, and Lpg0362 during phase transition, we analyzed their levels at different growth phases *via* proteomic analysis of whole lysates obtained from cultures of *L. pneumophila* WT at indicated time points. The results showed the lower levels of Lpg0102, Lpg0361, and Lpg0362 during the TP, whereas higher levels were detected upon entry into the RP (Fig. 5, *A–C*), which suggests that the expression of Lpg0102, Lpg0361, and Lpg0362 during the biphasic life cycle of *L. pneumophila* is growth phase dependent.

To determine whether the regulation of Lpg0102, Lpg0361, and Lpg0362 is associated with ClpP, we also measured their protein levels in the Δ*clpP* strain. During the TP, the levels of Lpg0102, Lpg0361, and Lpg0362 were significantly upregulated in the Δ*clpP* strain compared with the WT. In contrast, during the RP, the levels of Lpg0102, Lpg0361, and Lpg0362 were significantly downregulated in the Δ*clpP* strain compared with the WT. These data indicate that the temporal levels of Lpg0102, Lpg0361, and Lpg0362 are also regulated *via* the ClpP-dependent proteolytic pathway.

To verify the function of Lpg0102, Lpg0361, and Lpg0362 during the life cycle of *L. pneumophila*, ectopic expression

plasmids (*lpg0102*, *lpg0361*, and *lpg0362*) were constructed and then transformed into the WT and Δ*clpP* strain to create the WT/p*lpg0102*, WT/p*lpg0361*, WT/p*lpg0362*, Δ*clpP*/p*lpg0102*, Δ*clpP*/p*lpg0361*, and Δ*clpP*/p*lpg0362* strain, by the method we reported previously (61). Bacterial inoculum from the TP culture was used to measure the impact of Lpg0102, Lpg0361, and Lpg0362 on the whole life cycle. The results of the *in vitro* growth assay showed that compared with WT/pJB908 and Δ*clpP*/pJB908, the ectopic expression of Lpg0102, Lpg0361, and Lpg0362 did not affect the growth of the WT but significantly prolonged the lag phase ($p < 0.001$) and weakened the proliferation of the Δ*clpP* strain (Fig. 5*D*), indicating that the effects of Lpg0102, Lpg0361, and Lpg0362 may have been caused by the impaired ClpP-dependent proteolytic pathway.

Western blot analysis revealed that Lpg0102, Lpg0361, and Lpg0362 were more abundant at the RP than the TP in a new round of the life cycles of WT/p*lpg0102*, WT/p*lpg0361*, and WT/p*lpg0362*, demonstrating that their levels were life cycle dependent (Fig. 5*E*). However, in Δ*clpP*/p*lpg0102*, Δ*clpP*/p*lpg0361*, and Δ*clpP*/p*lpg0362*, the three proteins were more abundant at the TP than the RP, which was contrary to the results of ectopic expression in the WT. Liquid culture observation and quantitative analysis verified that during the prolonged lag phase of Δ*clpP*/p*lpg0102*, Δ*clpP*/p*lpg0361*, and Δ*clpP*/p*lpg0362*, the levels of
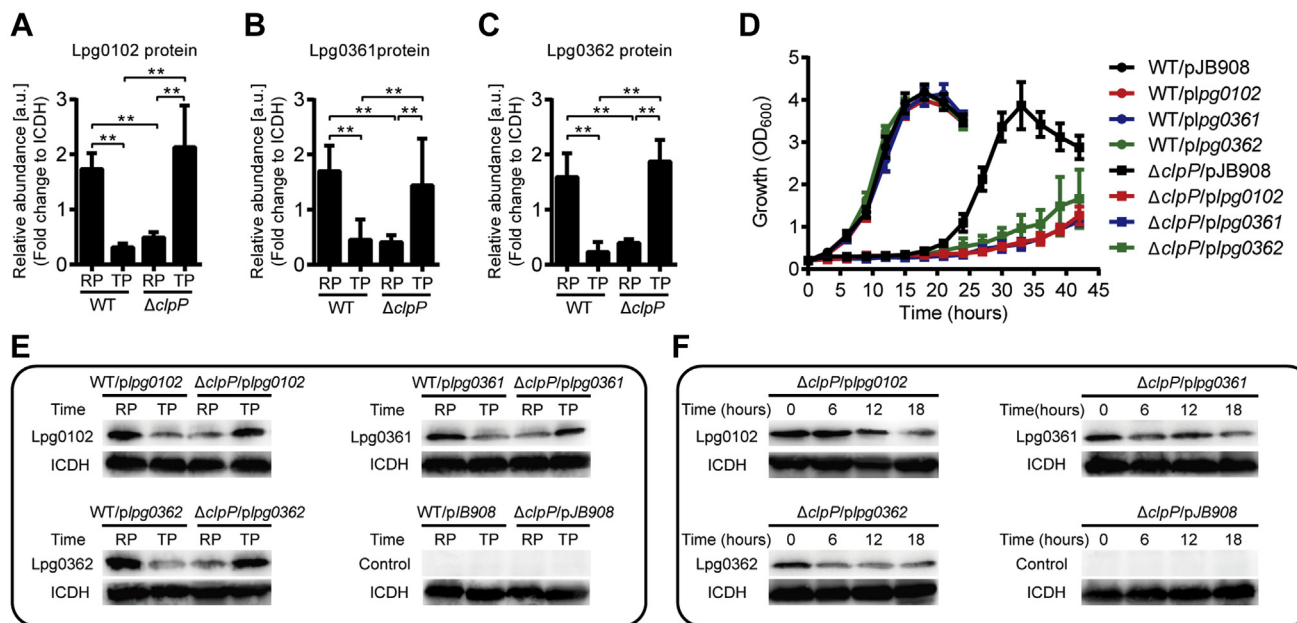
FIG. 5. **Accumulation of fatty acid biosynthesis–related proteins because of the loss of ClpP regulation delays the transition of** *Legionella pneumophila* from the transmissive phase (TP) into the replicative phase (RP). *A–C*, proteomics analysis of the protein levels of Lpg0102, Lpg0361, and Lpg0362 in WT and ΔclpP at indicated growth phases. WT and ΔclpP were separately cultured in fresh AYE medium at the same initial values of absorbance at 600 nm. Bacterial cells in the RP were harvested at an absorbance of 0.7 to 1.0 at 600 nm and that in the TP were harvested approximately 6 h after the cessation of growth. Total proteins from indicated samples were extracted for proteomic analysis, and the representative peptides were identified by mass spectrometry. ICDH was measured as control. Data represent mean ± SD derived from three independent experiments. **$p < 0.01$ were identified by GraphPad Prism. *D*, growth curves of *L. pneumophila* WT strain WT (●), WT with *lpg0102* expression (WT/p*lpg0102*) (●), WT with *lpg0361* expression (WT/p*lpg0361*) (●), WT with *lpg0362* expression (WT/p*lpg0362*) (●), the *clpP* deletion mutant ΔclpP (■), ΔclpP with *lpg0102* expression (ΔclpP/p*lpg0102*) (■), ΔclpP with *lpg0361* expression (ΔclpP/p*lpg0361*) (■), and ΔclpP with *lpg0362* expression (ΔclpP/p*lpg0362*) (■). For negative controls, pJB908 vector was electroporated into WT and ΔclpP to create WT/pJB908 and ΔclpP/pJB908, respectively. Bacterial strains in TP (absorbance at 600 nm = 3.0–3.5) were grown in AYE medium at 37 °C, and samples were taken every 3 h for determination of absorbance at 600 nm. Because only the *clpP* gene was knocked out based on the genomic resequencing, the complemented strain ΔclpP/C was not included in the experiments (61). *E*, ectopic protein levels of proteins Lpg0102, Lpg0361, and Lpg0362 at indicated growth phases. Bacterial whole-cell lysates from WT/p*lpg0102* and ΔclpP/p*lpg0102*, WT/p*lpg0361* and ΔclpP/p*lpg0361*, WT/p*lpg0362* and ΔclpP/p*lpg0362* were prepared, and an immunoblot of proteins was probed with an anti-His tag antibody. ICDH was measured as a loading control. RP refers to the exponential growth of bacteria in AYE broth, and TP refers to the period approximately 6 h after the cessation of growth. For negative controls, WT/p*JB908* and ΔclpP/p*JB908* were also measured. *F*, ectopic protein levels of proteins Lpg0102, Lpg0361, and Lpg0362 at time points indicated. Bacterial whole-cell lysates from ΔclpP/p*lpg0102*, ΔclpP/p*lpg0361*, and ΔclpP/p*lpg0362* were prepared, and an immunoblot of proteins was probed with an anti-His tag antibody. ICDH was measured as a loading control. The time points 0, 6, 12, and 18 h refers to the transition from TP to RP in rich medium. For negative controls, ΔclpP/p*JB908* was also measured. AYE, *N*-(2-acetamido)-2-aminoethanesulfonic acid–buffered yeast extract; ClpP, caseinolytic protease P; ICDH, isocitrate dehydrogenase.

Lpg0102, Lpg0361, and Lpg0362 in the *clpP* mutant gradually decreased, as its growth slowly recovered (Fig. 5, *D* and *F*), suggesting that the degradation of Lpg0102, Lpg0361, and Lpg0362 is ClpP dependent during the TP.

Overall, these findings demonstrate that the protein levels of Lpg0102, Lpg0361, and Lpg0362 are both life cycle dependent and temporally regulated in a ClpP-dependent manner during phase transition. In addition, the result that the accumulation of Lpg0102, Lpg0361, and Lpg0362 delays the transition from the TP to the RP added new evidence to understand part of the intermediates/proteins in the fatty acid biosynthesis–related pathways in the regulation of *L. pneumophila* life cycle.

ClpP Regulates SpoT Levels via Fatty Acid Biosynthetic Proteins to Mediate the TP to RP Transition

L. pneumophila is reportedly lacking in SpoT hydrolase activity, which impairs its transition from the TP to RP in either culture media or macrophages (29). Notably, SpoT-dependent stress response is associated with fatty acid metabolism (115, 116). Since the ectopic expression of three fatty acid biosynthesis–related proteins significantly prolonged the lag phase of the ΔclpP strain, we aimed to determine whether SpoT expression was also affected by these proteins. Hence, transcriptional analysis of *spoT* levels in the ΔclpP/pJB908, ΔclpP/p*lpg0102*, ΔclpP/p*lpg0361*, and ΔclpP/p*lpg0362* strains was performed using qRT–PCR. At each indicated time point, the transcriptional levels of *spoT* were significantly

lower in Δ*clpP*/p*lpg0102*, Δ*clpP*/p*lpg0361*, and Δ*clpP*/p*lpg0362* than in Δ*clpP*/pJB908 (Fig. 6*A*). However, the *spoT* expression in the three strains gradually increased relative to the growth progression (Fig. 6*A*), which contradicted the protein levels of Lpg0102, Lpg0361, and Lpg0362 (Fig. 5*F*). In the WT, *spoT* expression was upregulated during the TP to RP transition (24 h, 0 h) and the RP to TP transition (15 h, 18 h) (Fig. 6*B*), suggesting that SpoT is modulated in a life cycle–dependent manner and required for phase transition. These findings were consistent with previous studies reporting that SpoT expression is required throughout the *L. pneumophila* life cycle to mediate ppGpp turnover *via* its hydrolase and synthase activities (29, 30, 117, 118).

SpoT hydrolase activity is critical during the switch from the TP to RP (29). Furthermore, the SpoT-mediated response to fatty acid biosynthesis potentially requires interaction with ACP (29, 115). The Lpg0102 (FabF), Lpg0361 (FabB), and Lpg0362 (FabB) were already confirmed to be involved with the ACP metabolite (Fig. 6*C*). Notably, the ectopic expression of these proteins in the Δ*clpP* strain reduced the expression level of *spoT*, suggesting that the prolonged lag phase in the Δ*clpP* strain may have been due to the lack of SpoT. To confirm this hypothesis, we performed qRT–PCR to detect the *spoT* mRNA levels during the lag phase in the Δ*clpP* strain. Compared with the WT, the *spoT* expression was significantly downregulated in the Δ*clpP* strain at 0 h and the lag phase (6, 12, and 18 h) (Fig. 6*D*), suggesting that the temporal upregulation of SpoT expression *via* the ClpP-mediated pathway is essential for the TP to RP transition.

The *spoT* ectopic expression strains were also constructed for the WT (*i.e.*, WT/p*spoT*) and Δ*clpP* strain (*i.e.*, Δ*clpP*/p*spoT*). The *in vitro* growth assay showed that compared with
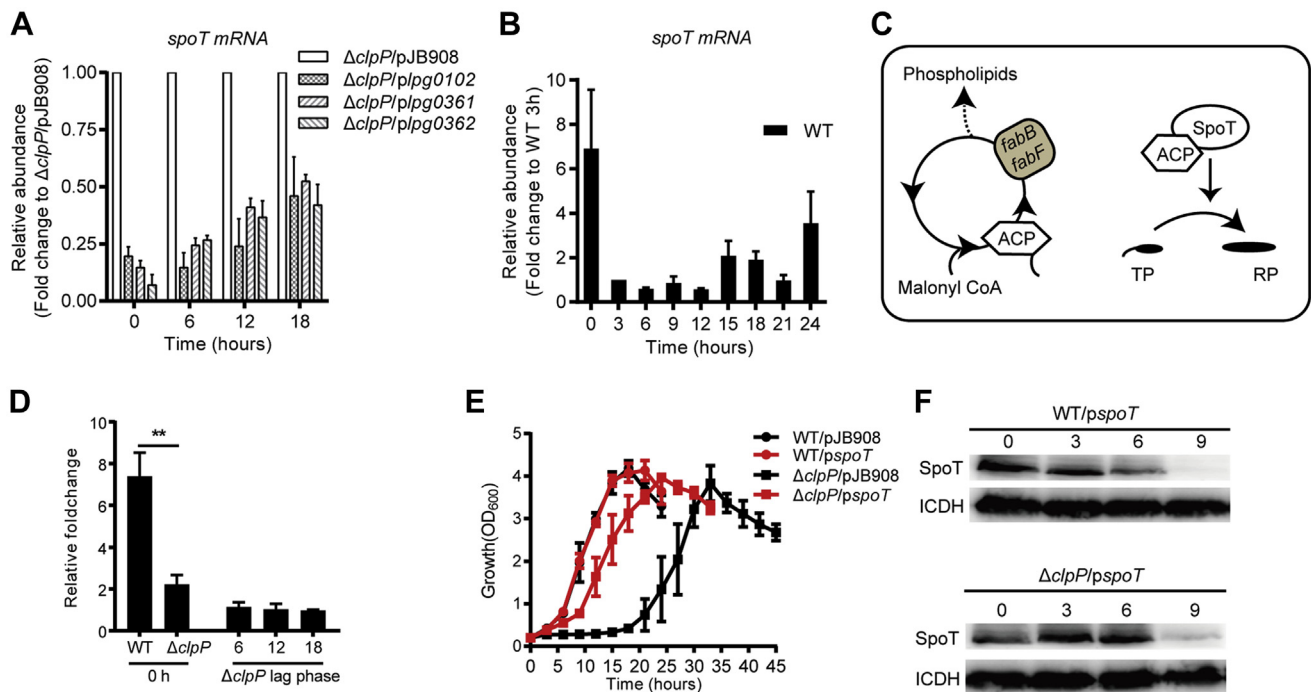

FIG. 6. **The lack of SpoT because of the loss of ClpP regulation delays the transition of *Legionella pneumophila* from the transmissive phase (TP) into the replicative phase (RP).** *A*, comparison of the transcriptional levels of *spoT* in Δ*clpP*, Δ*clpP*/p*lpg0102*, Δ*clpP*/p*lpg0361*, and Δ*clpP*/p*lpg0362* at time points indicated. The time points 0, 6, 12, and 18 h refers to the transition from TP to RP in rich medium. The transcriptional levels of *spoT* in Δ*clpP*/p*JB908* at each time points were normalized to 1.0. Data represent mean ± SD derived from three independent experiments. The transcriptional levels of *spoT* were significantly decreased (*p* < 0.01) in Δ*clpP*/p*lpg0102*, Δ*clpP*/p*lpg0361*, and Δ*clpP*/p*lpg0362* at each time points compared with Δ*clpP*/pJB908. *B*, transcriptional profile of *spoT* of WT. Total RNA was prepared from WT at the indicated time points. The transcriptional levels at 3 h were normalized to 1.0. *C*, schematic of fatty acid metabolism indicating where Lpg0102 (FabF), Lpg0361 (FabB), and Lpg0362 (FabB) act, and then SpoT monitors *L. pneumophila* differentiation likely through an interaction with acyl-carrier protein (ACP) (115). *D*, transcriptional profile of *spoT* in WT at 0 h and in Δ*clpP* at 0, 6, 12, and 18 h (lag phase of Δ*clpP* strain). Total RNA was prepared from WT at the indicated time points. *E*, growth curves of *L. pneumophila* WT strain WT (●), WT with *spoT* expression (WT/p*spoT*) (●), the *clpP* deletion mutant Δ*clpP* (■), and Δ*clpP* with *spoT* expression (Δ*clpP*/p*spoT*) (■). For negative controls, pJB908 vector was electroporated into WT and Δ*clpP* to create WT/pJB908 and Δ*clpP*/pJB908, respectively. Bacterial strains in TP (absorbance at 600 nm = 3.0–3.5) were grown in AYE medium at 37 °C, and samples were taken every 3 h for determination of absorbance at 600 nm. *F*, ectopic protein levels of protein SpoT at indicated growth phases. Bacterial whole-cell lysates from WT/p*spoT* and Δ*clpP*/p*spoT* were prepared, and an immunoblot of proteins was probed with an anti-His tag antibody. ICDH was measured as a loading control. The time points 0, 3, 6, and 9 h refers to the transition from TP to RP in rich medium. AYE, *N*-(2-acetamido)-2-aminoethanesulfonic acid–buffered yeast extract; ClpP, caseinolytic protease P; ICDH, isocitrate dehydrogenase.

WT/pJB908 and ΔclpP/pJB908, the ectopic expression of SpoT did not affect the growth of the WT but significantly recovered from the lag phase (>80%) and enhanced the proliferation of the ΔclpP strain (Fig. 6E). Western blot analysis of the SpoT levels at indicated time points revealed that in a new round of WT/pspoT life cycle, SpoT levels were detected during the TP and TP to RP transition but were downregulated upon the shift into RP (Fig. 6F). In ΔclpP/pspoT, SpoT levels were detected during the TP, upregulated during the TP to RP transition (0 to 3 h), and downregulated upon entry into the RP. Furthermore, the ectopic expression of RelA (another trigger of the stringent response that follows fluctuations in amino acid availability (23, 33)) in the ΔclpP strain did not recover the lag phase (data not shown).

Overall, these results demonstrate that the functional loss of ClpP resulted in the accumulation of fatty acid biosynthesis–related proteins, and the downregulation of SpoT expression delayed the transition from the TP to RP. Thus, *L. pneumophila* requires ClpP-dependent proteolysis to monitor fatty acid biosynthesis–related proteins and SpoT expression for the normal regulation of microbial differentiation.

Regulation of the Biphasic Life Cycle and Bacterial Virulence is Independent

We previously observed that the deletion of *clpP* not only delays the entry to the RP but also impairs bacterial infectivity to the host and inhibits the proliferation ability in cells (59–61). To investigate whether the levels of Lpg0102, Lpg0361, Lpg0362, and SpoT influenced bacterial infectivity, *L. pneumophila* strains in the TP were exposed to amoebae *A. castellanii* for 2 h. The extracellular bacteria were subsequently cleared, and the amoebae were lysed to release *L. pneumophila* and calculate CFU of the infectious bacteria. The results showed that the survival capabilities of WT/plpg0102, WT/plpg0361, WT/plpg0362, and WT/pspoT were similar to that of WT after phagocytosis (Fig. 7, A and B). However, the survival capabilities of ΔclpP/plpg0102, ΔclpP/plpg0361, ΔclpP/plpg0362, and ΔclpP/pspoT were significantly lower than that of ΔclpP harboring only the empty vector. Furthermore, the proliferation rates of the WT with lpg0102, lpg0361, lpg0362, and spoT ectopic expression were identical to that of the WT, whereas the proliferation of the ΔclpP strains with and without ectopic expression was consistently inhibited (Fig. 7, C and D). Comparing the survival and proliferation abilities of ΔclpP/plpg0102, ΔclpP/plpg0361, and ΔclpP/plpg0362 with their growth curves (Figs. 5D, 7, A and C), the ectopic expression of SpoT *in vitro* almost completely recovered the transition of the life cycle and strengthened the proliferation of the ΔclpP strain (Fig. 6E); however, the proliferation ability of ΔclpP/pspoT *in vivo* did not improve, and its survival capability *in vivo* was further impaired (Fig. 7, B and D). These results suggest that the

regulation of the biphasic life cycle and bacterial virulence is independent.

Thus, our data complemented and improved the existing model (18). Particularly, our model showed that the regulation of SpoT might be more vital than other regulator proteins for the progress of biphasic life cycle, and the regulation of more than 120 ClpP-dependent phase-specific effectors identified in this study provide new insights into the independent regulation of bacterial virulence.

Several T4BSS and Effector Proteins are Regulated in a ClpP-Dependent Manner During the Biphasic Life Cycle

During the RP, *L. pneumophila* cannot initiate infection to macrophages and avoid fusion with lysosomes. During the TP, the bacterial pathogen can effectively infect the macrophages, departing from the endocytic pathway shortly after internalization to establish a replicative vacuole (119). This indicates that the abundance of effectors at different stages is essential for normal function at a specific period. Notably, we observed that the protein levels of several Dot/Icm effectors at different phases were dependent on ClpP, including 93 RP-specific and 52 TP-specific effectors (Fig. 2 and supplemental Table S17).

Compared with the WT, 44 and 49 effectors were downregulated and upregulated, respectively, in the RP of the ΔclpP strain (Fig. 8, A and B). The downregulated effectors include LnaB (an *L. pneumophila* activator of NF-κB) (120), LegC8/Lgt2 (an *L. pneumophila* glucosyltransferase might be necessary for egress of the bacteria from the host cell) (121, 122), SidE (catalyzes the noncanonical ubiquitination of several substrate proteins (123, 124)), and SidP (a PI-3-phosphatase that specifically hydrolyzes PI[3]P and PI[3,5]P2 *in vitro*) (125). The upregulated effectors consist of MavQ (a phosphoinositide 3-kinase that specifically catalyzes the conversion of phosphatidylinositol [PtdIns] into PtdIns3P) (126), LepA (promotes nonlytic release of *L. pneumophila* from protozoa) (127, 128), RidL (inhibits retromer function to promote intracellular bacterial replication) (129), LegC7/YlfA (located in the endoplasmic reticulum–derived replicative vacuole at later stage of a host cell infection) (130, 131), LpnE (required for efficient host cell entry) (132–134), SdeA and SdeC (members of the SidE effector family) (123, 124), RalF (a guanine nucleotide exchange factor activating ADP-ribosylation factor on LCVs) (49, 135), LegC3 (inhibits vacuole fusion) (136, 137), RavZ (inhibits autophagy during infection) (138), Lem10/Lpg1496 (potentially plays a role in nucleotide metabolism) (139), Lgt1 (a GT-A type glucosyltransferase family protein inhibits protein synthesis) (140–143), LupA (catalyzes the removal of ubiquitin from target proteins) (144), RavK (disrupts host cytoskeletal structure by cleaving actin) (145), SidK (specifically targets host v-ATPase and reduces phagosomal acidification and promotes survival of the bacterium inside macrophages) (146, 147), LidA (disrupts the switch function of Rab1 to render it persistently active) (148,
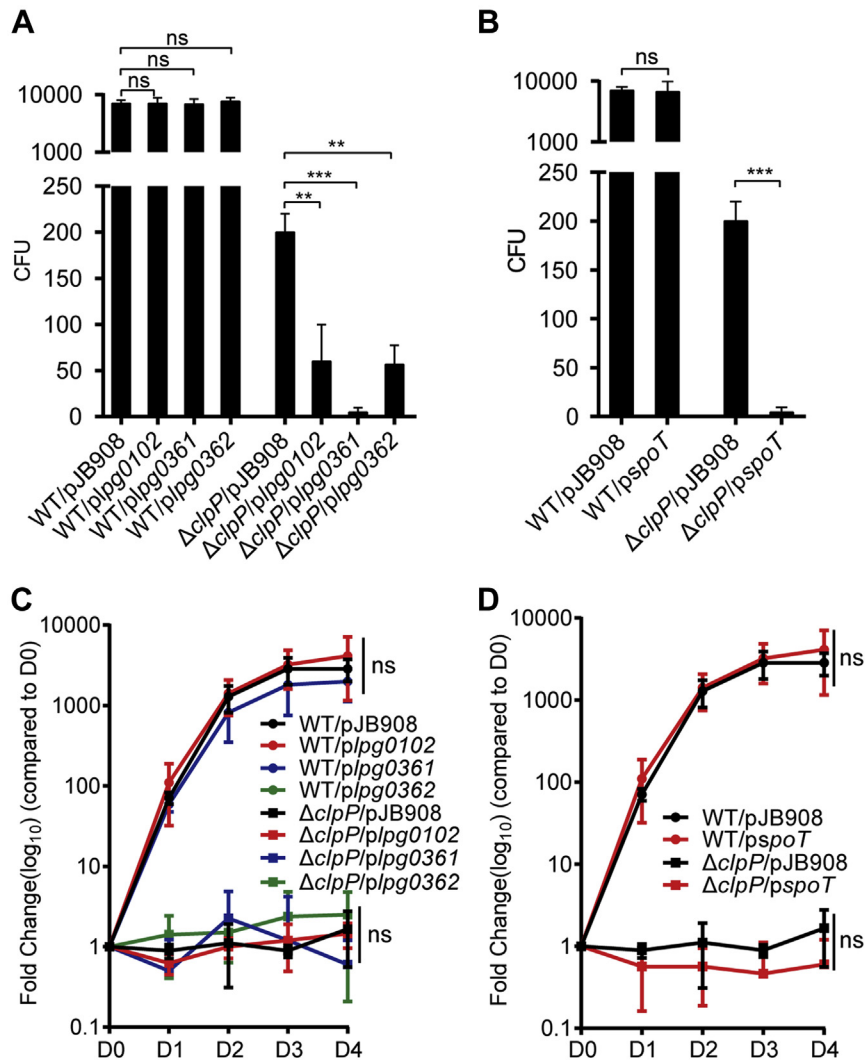
FIG. 7. **Ectopic expression of fatty acid metabolism proteins and SpoT reduces the viability of Δ*clpP* strain in host cells.** *A* and *B*, *Acanthamoeba castellanii* were infected with transmissive phase (TP) strains WT/pJB908, Δ*clpP*/pJB908, at a multiplicity of infection of 10. pJB908 vector can express the thymine required for growth of bacteria *in vivo*. Viability of strains WT/p*lpg0102*, WT/p*lpg0361*, WT/p*lpg0362*, Δ*clpP*/p*lpg0102*, Δ*clpP*/p*lpg0361*, and Δ*clpP*/p*lpg0362* was shown in supplemental Fig. S8*A*, and the viability of strains WT/p*spoT* and Δ*clpP*/p*spoT* was shown in supplemental Fig. S8*B*. Thirty minutes postinfection, extracellular bacteria were removed by washing with warm HL5 medium three times. Infected amoebae cells were lysed after 90 min, and intracellular bacteria were quantified by determining the colony-forming unit (CFU). Each time point represents the mean ± SD from three independent experiments. The quantitative data were analyzed using two-way ANOVA test by GraphPad Prism. The values that are significantly different are indicated by a *bar* and *asterisk* as follows: **$p <$ 0.01, ***$p <$ 0.001. ns means no difference from the WT. *C* and *D*, intracellular growth kinetics of WT/p*lpg0102* (●), WT/p*lpg0361* (●), WT/p*lpg0362* (●), Δ*clpP*/p*lpg0102* (■), Δ*clpP*/p*lpg0361* (■), and Δ*clpP*/p*lpg0362* (■) in *A. castellanii* and the intracellular growth kinetics of WT/p*spoT* (●) and Δ*clpP*/p*spoT* (■) in *A. castellanii*. Amoebae cells were seeded into 24-well plates and infected with *Legionella pneumophila* at a multiplicity of infection of 10. At each time point indicated, amoebae cells were lysed, and the colony-forming unit was determined by plating dilutions onto BCYE plates. Infections were performed at 30 °C. BCYE, buffered charcoal yeast extract; ClpP, caseinolytic protease P.

149), and VipA (involved in actin binding and polymerization and interferes with eukaryotic organelle trafficking) (150).

Compared with the WT, 31 and 21 effectors were down-regulated and upregulated, respectively, in the TP of the Δ*clpP* strain (Fig. 8, *C* and *D*). The downregulated effectors include VipD (a phospholipase A that blocks endosome fusion with LCVs) (151–153), SidC (accumulates during the TP; after anchoring to phosphatidylinositol-4 phosphate on the LCVs,

supports efficient intracellular growth and recruitment of endoplasmic reticulum–derived vesicles to the LCV) (154–156), SdcA (a paralog of SidC; the gene is localized directly upstream of *sidC*) (154, 155), SidD (a deAMPylase for Rab1 modification) (157, 158), SidM/DrrA (a Rab1 guanine nucleotide exchange factor that regulates the transport of endoplasmic reticulum–derived vesicles and binds to phosphatidylinositol-4 phosphate) (159–162), SidG (translocation into host cells is highly
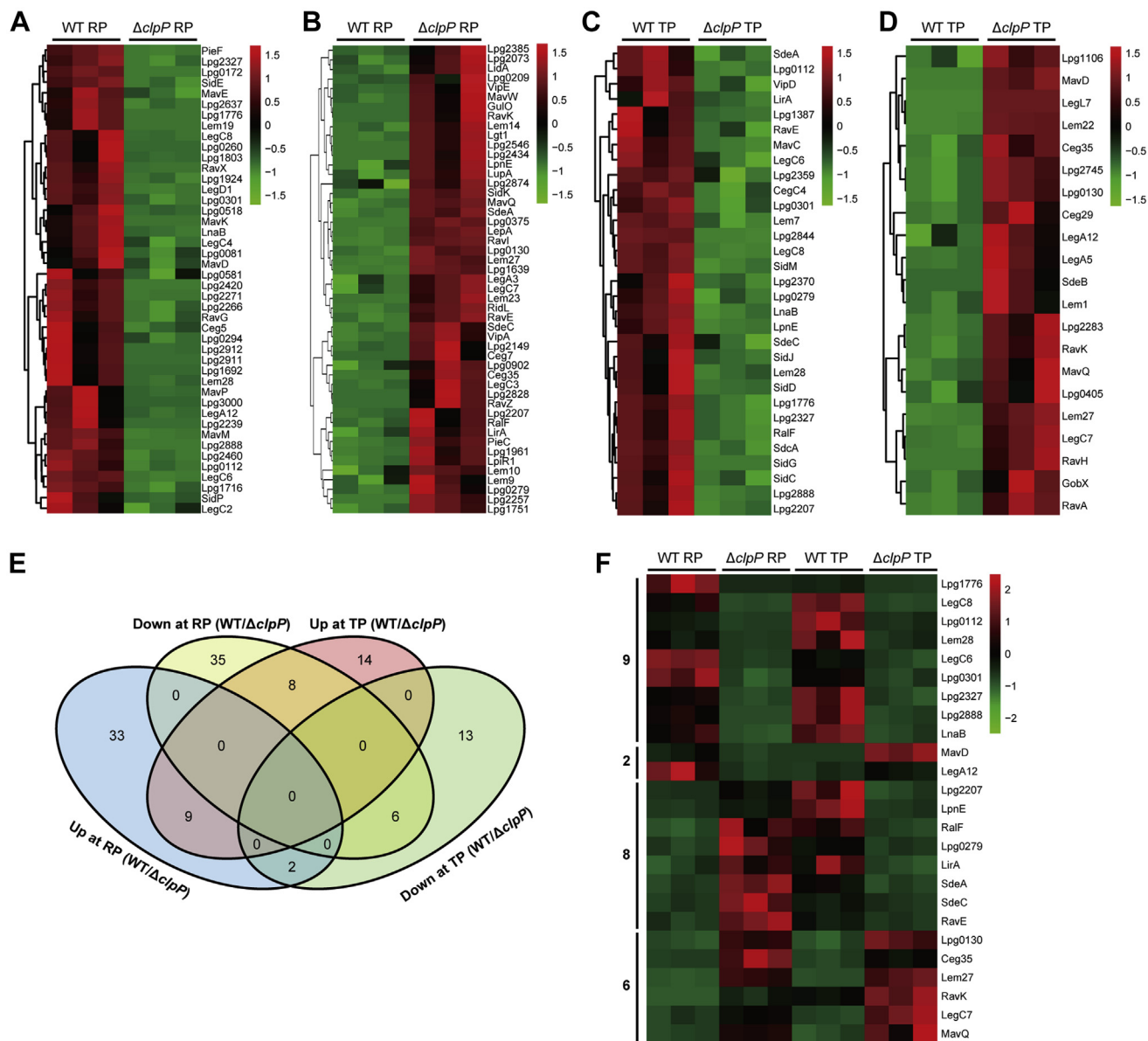
FIG. 8. **The dynamics of abundance of many effector proteins is regulated by ClpP-dependent proteolysis at the replicative phase (RP) and the transmissive phase (TP).** *A*, heatmap analysis showed that 44 effectors were downregulated in the Δ*clpP* strain at the RP (*i.e.*, more abundant in the WT at the RP). *B*, heatmap analysis showed that the 49 effectors were upregulated in the Δ*clpP* strain at the RP (*i.e.*, less abundant in the WT at the RP). *C*, heatmap analysis showed that 31 effectors were downregulated in the Δ*clpP* strain at the TP (*i.e.*, more abundant in the WT at the TP). *D*, heatmap analysis showed that 21 effectors were upregulated in the Δ*clpP* strain at the TP (*i.e.*, less abundant in the WT at the TP). *E*, Venn diagram displayed the effectors that were regulated at both the RP and the TP. *F*, heatmap analysis showed the effectors that were regulated at both the RP and the TP. ClpP, caseinolytic protease P.

dependent on IcmS and IcmW proteins) (163), SidJ (required for efficient recruitment of endoplasmic reticulum proteins to the bacterial phagosome) (164), LegC8, LnaB, LpnE, RalF, SdeA, and SdeC. The upregulated effectors consist of GobX (exploits host cell S-palmitoylation to gain accurate host subcellular targeting) (165), LegA5 (a phosphatidylinositol 3-kinase that catalyzes the formation of PtdIns3P from PtdIns) (166), RavK, LegC7/YlfA, and MavQ.

We also observed that several ClpP-dependent effectors were regulated during both the RP and TP (Fig. 8*E*). In the absence of ClpP, the levels of various effectors varied depending on the phase: nine (Lpg1776, LegC8/Lgt2, Lpg0112, Lem28, LegC6, Lpg0301, Lpg2327, Lpg2888, and LnaB) were downregulated at both the RP and TP; two (MavD and LegA12) were downregulated at the RP but upregulated at the TP; eight (Lpg2207, LpnE, RalF, Lpg0279, LirA, SdeA,

SdeC, and RavE) were upregulated at the RP but down-regulated at the TP; and six (Lpg0130, Ceg35, Lem27, RavK, LegC7, and MavQ) were upregulated both at the RP and TP (Fig. 8F). Interestingly, several components of the Dot/Icm apparatus, which is critical for *L. pneumophila* virulence (167, 168), were also regulated *via* the ClpP-dependent proteolytic pathway. Among these, six Dot/Icm apparatus core complex proteins (DotK, DotH/IcmK, DotU/IcmH, IcmL-like/Lpg0708, DotA, and IcmV) were expressed at the RP, whereas four (DotI/IcmL, DotU/IcmH, DotC, and IcmV) were expressed at the TP (Fig. 2, supplemental Tables S11 and S12). Notably, *L. pneumophila* loses its virulence and infectivity without DotA (169). Taken together, these findings suggest that the ClpP-dependent proteolysis of T4BSS and effector proteins during the biphasic life cycle is vital for *Legionella* pathogenesis.

ClpP Directly Controls Several Substrates Associated with the Biphasic Life Cycle and Bacterial Virulence

Regulated proteolysis is the specific and conditional degradation of substrate proteins that allows the downstream controlled proteins to regulate cellular adaptations and differentiations in response to extracellular or intracellular signals (50–55). To identify the substrates of ClpP, we performed an *in vivo* experiment using a proteolytic inactive form of ClpP (ClpP^{trap}) that retains but does not degrade the substrates that translocate into the proteolytic chamber, as we and others reported previously (61, 62, 170, 171). The plasmids expressing His-tagged ClpP^{wt} and ClpP^{trap} were transformed into the Δ*clpP* strain to create Δ*clpP*/p*clpP*^{wt} and Δ*clpP*/p*clpP*^{trap}, respectively. Since the His-tagged ClpP^{wt} in this strain has an intact active site, substrates will be degraded upon entry into the ClpP-proteolytic chamber; hence, the proteins that are copurified with the ClpP^{trap} but are not captured by ClpP^{wt} represent ClpP substrates (Fig. 1C). Substrates captured inside the proteolytic barrel were copurified with the His-tagged ClpP complex and identified by MS (61, 62, 170, 171).

A total of 76 proteins captured by ClpP^{trap} were identified (Table 3). Several proteins were previously identified as substrates of the Clp protease in other bacteria (62), such as Pgi (glucose-6-phosphate isomerase), PanC (pantothenate synthetase), and GatB (aspartyl/glutamyl-tRNA[Asn/Gln] amidotransferase subunit B). On the other hand, a large number of substrates was not described before. Interestingly, 37 ClpP-regulated proteins were also captured by the ClpP^{trap}, demonstrating that the repeated capture of known ClpP substrates and unstable proteins verifies that the ClpP substrates were specifically copurified with the ClpP^{trap}. The identified ClpP substrates included 19 phase-specific proteins, namely Pgi, PanB, MreC, CydA, CsrA, FlhF, RavE, SdeC, ClpS, ProQm/Lpg0133, Lpg1446, Lpg0248, Lpg0773, Lppg2440, Lpg2948, Lpg1993, Lpg2724, Lpg1102, and Lpg0953, and six effectors (Lem19, LegD1, Lem22, RavE, MavQ, and SdeC). These results suggest that ClpP also is

directly involved in the regulation of *L. pneumophila* life cycle and virulence.

In addition, we found that two fatty acid biosynthesis–related substrates, WaaM/Lpg0363 (lipid A biosynthesis acyltransferase) and LipB/Lpg1511, showed high confidence values in the interaction with Lpg0102, Lpg0361, and Lpg0362 (supplemental Fig. S13, A and B). A model of the hierarchical position of ClpP in the regulatory network suggests that ClpP directly regulates the abundance of WaaM and LipB and indirectly controls the protein levels of Lpg0102, Lpg0361, and Lpg0362, which then monitors the SpoT expression levels, thereby completing the regulation of *L. pneumophila* differentiation (supplemental Fig. S13C). Moreover, we have demonstrated that ClpP modulates the level of substrate protein CsrA *via* direct degradation during the TP, consequently facilitating the progress of the biphasic life cycle of *L. pneumophila* (61). These results exhibit that ClpP-dependent proteolysis can specifically and conditionally degrade substrate proteins, either to directly perform a regulatory role or to indirectly control cellular events by regulating the abundance of controlled proteins.

We finally compared the life cycle proteome data with the ClpP^{trap} data and discussed the crosstalk of the regulatory elements that govern *L. pneumophila* life cycle and virulence in a ClpP-dependent manner using a systems view. The comparison provides testable hypotheses and putative substrates for further determining the significance of ClpP-driven proteolysis (Fig. 9).

DISCUSSION

The fine-tuned control of biphasic life cycle and temporal delivery of approximately 330 effector proteins into host cells enables *L. pneumophila* to adapt to changing intracellular and extracellular environments for surviving and proliferation (5–7). Thus, the life cycle–dependent regulation of necessary proteins is required for their function (8, 9). In this study, we present a comprehensive proteomic profile on the life cycle–dependent proteins that are regulated by ClpP-mediated proteolysis (Table 1 and Fig. 3) and report the temporal regulation of effector expression *via* the ClpP proteolytic pathway (Fig. 8). On a proteomic scale, our data will help to further understand the underlying mechanisms that regulate the phase-specific proteins of this highly adaptive pathogen.

Comparison of the protein levels between the RP and TP revealed that 428 proteins, including 220 that were upregulated in the RP and 208 that were upregulated in the TP, were significantly differentially expressed (Table 1 and supplemental Fig. S1). This trend corroborates the results of a previous study, in which 176 proteins were identified as upregulated in the RP and 147 were upregulated in the TP *via* an LC–MS-based proteomic analysis (14). As expected, a high overlap in the identified RP- and TP-specific proteins was observed between our study and by Aurass *et al.* (14). The

TABLE 3

The identified substrates of ClpP in L. pneumophila

Protein name	Gene ID	MW (kDa)	Calc (pl)	RP ratio[a]	TP ratio[b]	WT abundance[c] Log2 (RP/TP)	Description
ClpS	lpg0817	12.7	5.45	1.19	3.27	1.90	ATP-dependent Clp protease adapter ClpS
FlhF	lpg1784	42.7	7.18	5.90	2.15	−2.76	Flagellar GTP-binding protein FlhF
MavQ	lpg2975	100.7	6.61	2.11	3.13	—	Uncharacterized protein
RavE	lpg0195	37.7	6.34	3.41	−1.31	−1.46	Uncharacterized protein
SdeC	lpg2153	172.3	6.34	3.40	−1.09	−1.38	Sid-related protein-like
CydA	lpg0199	51.1	8.24	2.28	−1.36	−1.07	Cytochrome D ubiquinol oxidase subunit I
Lpg1279	lpg1279	13.5	9.63	1.48	—	—	Uncharacterized protein
YqkA	lpg1614	36.9	7.91	1.66	—	—	Glutamate-rich protein GrpB
Lpg1993	lpg1993	33.3	8.76	3.02	—	−1.81	Polysaccharide deacetylase
Lpg2724	lpg2724	13.4	4.56	1.31	—	−1.41	Uncharacterized protein
Lpg0248	lpg0248	13	7.34	1.20	—	−1.52	Arsenate reductase
Lpg2440	lpg2440	39.7	8.32	2.87	—	−1.84	Glutathione-*S*-transferase
Lpg0953	lpg0953	63.3	7.39	1.56	—	−1.87	AMP-binding protein
Lpg1102	lpg1102	33.4	6.46	2.31	—	−1.14	Uncharacterized protein
PanB	lpg2661	28.6	6.98	1.66	—	−1.51	3-Methyl-2-oxobutanoate hydroxymethyltransferase
Lpg0737	lpg0737	15.5	9.8	1.34	—	—	Hypothetical signal peptide protein
Lpg0659	lpg0659	64.4	8.22	1.21	—	—	ABC transporter ElsE
Tdk	lpg0636	24	5.64	8.00	—	—	Thymidine kinase
Lpg2386	lpg2386	21.8	5.3	1.21	—	—	Uncharacterized protein
Lpg2948	lpg2948	12.3	5.74	−4.88	—	5.83	Uncharacterized protein
Lpg1476	lpg1476	11.4	7.2	−1.62	—	—	Uncharacterized protein
Lem19	lpg2166	49.2	6.81	−4.69	—	—	Uncharacterized protein
LegD1	lpg2694	33	5.73	−3.69	—	—	Phytanoyl-CoA dioxygenase
Lpg0567	lpg0567	53.7	10.01	−2.32	—	—	Peptidase, M23/M37 family
Lpg0007	lpg0007	31.9	5.78	−1.76	—	—	Probable hydrolase
MreC	lpg0812	33.4	8.25	−5.38	2.11	3.06	Cell shape–determining protein MreC
Lpg1446	lpg1446	22.6	5.07	—	2.54	3.16	Segregation and condensation protein B
ProQm	lpg0133	25.7	9.99	—	3.53	3.85	RNA chaperone ProQ
Pgi	lpg0759	56.1	6.34	—	3.67	3.51	Glucose-6-phosphate isomerase
Lpg0773	lpg0773	53.9	8.81	—	1.96	2.51	Polysaccharide ABC transporter
CsrA	lpg1593	7.4	7.42	—	2.06	1.41	Carbon storage regulator CsrA
Lem22	lpg2328	14.7	6.02	—	2.22	—	Uncharacterized protein
AroF	lpg2530	38.9	7.23	—	5.29	—	Phospho-2-dehydro-3-deoxyheptonate aldolase
Lpg0906	lpg0906	18.5	4.97	—	2.10	—	Flagellar biosynthesis
Lpg1066	lpg1066	21.1	6.8	—	2.04	—	Uncharacterized protein
Lpg2763	lpg2763	47	6.54	—	−4.31	—	Mg^{2+} and Co^{2+} transporter CorB, hemolysin
WaaM	lpg0363	32.7	9.96	—	−1.46	—	Lipid A biosynthesis acyltransferase
Lpg0065	lpg0065	31.7	5	—	—	3.11	Uncharacterized protein
MavV	lpg2638	52.9	6.06	—	—	8.00	Uncharacterized protein
Lpg2160	lpg2160	55.9	5.86	—	—	−3.51	Uncharacterized protein
Lpg1810	lpg1810	52.6	6.47	—	—	−1.21	Long chain fatty acid transporter
RpsT	lpg2636	9.7	11.36	—	—	2.99	30S ribosomal protein S20
Lpg0229	lpg0229	31.8	6.39	—	—	—	Heme oxygenase
UppS	lpg0503	27.4	6.3	—	—	—	Polycis-undecaprenyl-diphosphate synthase
Lpg0732	lpg0732	23.4	6.07	—	—	—	Uncharacterized protein
Lpg0839	lpg0839	20.3	5.57	—	—	—	KdsC
PilZ	lpg1401	12.5	8.27	—	—	—	Type 4 fimbrial biogenesis protein PilZ
Lpg2717	lpg2717	18.2	7.58	—	—	—	Uncharacterized protein
FolE2	lpg2766	21.1	7.01	—	—	—	GTP cyclohydrolase 1
LipB	lpg1511	22.7	7.64	—	—	—	Octanoyltransferase
PilQ	lpg0931	77.4	8.95	—	—	—	Type IV pilus biogenesis protein PilQ
Lpg0469	lpg0469	29.5	8.88	—	—	—	Phosphatase family protein
Lpg0466	lpg0466	66.4	5.64	—	—	—	Oxaloacetate decarboxylase alpha subunit
BamE	lpg0372	13.2	10.33	—	—	—	Small protein A, tmRNA-binding
DsbD	lpg0686	65.3	8.68	—	—	—	Thiol:disulfide interchange protein DsbD
Lpg0594	lpg0594	7.2	3.93	—	—	—	Uncharacterized protein
FrgA	lpg2800	67.2	8.12	—	—	—	Siderophore biosynthetic protein FrgA
Lpg1291	lpg1291	53.3	6.71	—	—	—	Two-component sensor kinase

Table 3—*Continued*

Protein name	Gene ID	MW (kDa)	Calc (pI)	RP ratio[a]	TP ratio[b]	WT abundance[c] Log2 (RP/TP)	Description
SurE	lpg1282	27	5.57	—	—	—	5′-Nucleotidase SurE
Lpg0730	lpg0730	38.7	9.07	—	—	—	Transmembrane permease
Lpg0525	lpg0525	23.5	5.74	—	—	—	Hypothetical virulence protein
IcmQ	lpg0444	22.4	9.52	—	—	—	IcmQ
Lpg0050	lpg0050	32.5	7.68	—	—	—	Integral membrane protein
Lpg0672	lpg0672	28.3	5.66	—	—	—	Acetoacetate decarboxylase ADC
PcoA	lpg1035	115.5	9.17	—	—	—	Copper efflux ATPase
RibE	lpg1178	22.3	5.96	—	—	—	Riboflavin synthase, alpha subunit RibE
PilB	lpg1522	62.7	5.85	—	—	—	(Type IV) pilus assembly protein PilB
Lpg1675	lpg1675	37.8	5.44	—	—	—	PurC
GatB	lpg1737	53.6	5.95	—	—	—	Asn/Gln amidotransferase subunit B
Lpg1795	lpg1795	29.2	9.25	—	—	—	Oxidoreductase
UgpQ	lpg2274	27.4	7.18	—	—	—	Glycerophosphoryl diester esterase
HypA	lpg2476	12.7	8	—	—	—	Hydrogenase maturation factor HypA
PanC	lpg2662	28.8	6.61	—	—	—	Pantothenate synthetase
SecG	lpg2791	10.4	9.88	—	—	—	Protein-export membrane protein SecG
YhiP	lpg2805	56.1	8.48	—	—	—	Peptide transport protein, POT family
Lpg1927	lpg1927	10.5	8.43	—	—	—	Probable Fe($^{2+}$)-trafficking protein

[a]Proteins with different abundances in the ΔclpP strain compared with the WT at the RP that are upregulated or downregulated, respectively, which are above or below the threshold of +1 and −1 log2(ΔclpP/WT).

[b]Proteins with different abundances in the ΔclpP strain compared with the WT at the TP that are upregulated or downregulated, respectively, which are above or below the threshold of +1 and −1 log2(ΔclpP/WT).

[c]Differentially expressed proteins of *L. pneumophila* WT at the RP and TP, which were above or below the threshold of +1 (RP-specific) and −1 (TP-specific) log2(RP/TP). (−) means no significant difference between the two groups.

striking feature of *L. pneumophila* is that actively replicating cells are nonmotile, whereas virulent cells are motile (6, 7). Similar to a previous report, cell division proteins (FtsA, FtsQ, FtsZ, and MreC) were observed to be more abundant at the RP, whereas proteins associated with flagellar assembly were more abundant at the TP (MotA, FlgH, FlgI, FlgA, FlhF, Lpg0907, FliA, FliS, and PilM), which contradict previous results (FliA, FlgD, FlgE, FlgK, FliD, and FliC) (14). We also discovered that 24 ribosomal proteins were more abundant at the RP, whereas Aurass *et al.* (14) reported that >20 ribosomal proteins were identified with high abundance both at the RP and TP. This discrepancy may have been due to the differences in the time of sample collection (at 6 h after the cessation of growth *versus* at 13.5 h when the bacteria were entering the TP and still growing) (11, 61). In addition, the expression profile of the identified proteins in our proteomic analysis was also consistent with those of previous transcriptional studies (10, 11), including the RP-specific proteins related to amino and sugar metabolism, cell division and biosynthetic processes, and the TP-specific proteins associated with virulence and survival (*e.g.*, Dot/Icm-translocated effectors and motility machinery [flagellar and type IV pilus genes]).

Clp proteases are powerful molecular machines that contribute to protein homeostasis during balanced growth, stress responses, and specific pathway regulation (50–55). Our previous findings showed that *clpP* deletion delays the transition of the biphasic life cycle of *L. pneumophila* and impairs bacterial survival and proliferation in host cells (59–61).

In the present study, we identified the ClpP-regulated proteins that are involved in the aforementioned phenotypes, especially the proteins involved in the stringent response network for governing *L. pneumophila* differentiation (*e.g.*, IHF, LqsR, FliA, PmrA, RpoS, LetE, and CsrA) and the effectors associated with virulence (*e.g.*, RalF, LepA, LpnE, LegC7/YlfA, VipA, VipD, and SidM/DrrA), which are consistent with the previous reports for other bacteria. For instance, ClpP in *Staphylococcus aureus* is also involved in the regulation of bacterial growth, stress tolerance, intracellular replication, and virulence (172–174). Another study on *Streptococcus mutans* reported that ClpP differentially regulates the expression of proteins involved in genomic islands, mutacin production, and antibiotic tolerance (175). In *Enterococcus faecalis*, ClpP participates in stress tolerance, biofilm formation, antimicrobial tolerance, and virulence (176). Notably, our proteomic data revealed that among the 428 differentially expressed proteins during the RP and TP in *L. pneumophila*, 316 (73.83%) were regulated *via* ClpP-dependent proteolysis, indicating that ClpP is a major determinant of the biphasic life cycle–dependent protein turnover (Fig. 3). The ClpP-regulated proteins involved in cell division and replication in *L. pneumophila* (*e.g.*, FtsZ, an essential component of the cell division machinery) were also observed in *E. coli* and *Caulobacter* (177–179), and those involved in phase transition (*e.g.*, RpoS, an alternative sigma factor that can compete with σ70 during stationary phase) were also found in *E. coli* (180). The role of regulated proteolysis in cell cycle progression has also been reported in other bacteria. In the aquatic dimorphic organism *Caulobacter*
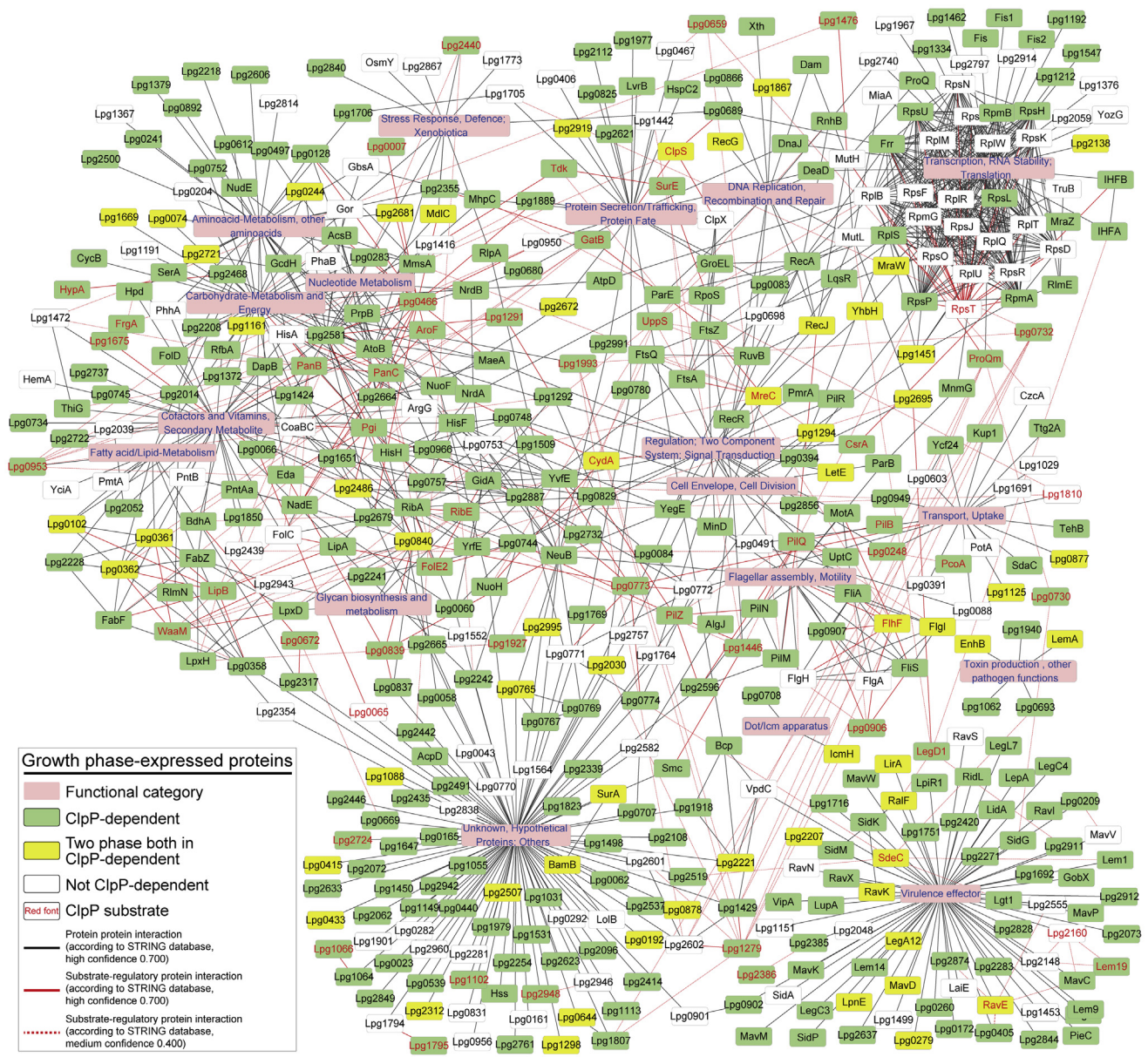
FIG. 9. **Systems view of growth stage–specific expressed proteins and substrate proteins regulated in a ClpP-dependent manner.** Integrated network of growth phase–dependent protein expression profiles mediated by ClpP. The life cycle proteome data were further compared with the ClpP^{trap} data and the STRING database to indicate protein interaction network reveal that ClpP-dependent proteolysis can specifically and conditionally degrade substrate proteins, either to directly perform a regulatory role or to indirectly control cellular events by regulating the abundance of regulatory proteins. Because of the complexity of the network and the secondary regulatory effects of proteins, the levels of life stage–specific proteins were regulated in a ClpP-dependent manner during both phases, which suggested a more potentially important role for the maintenance of biphasic life cycle. ClpP, caseinolytic protease P.

crescentus, ClpP regulates the transition from swarmer to stalked phenotype (181). In *E. coli*, ClpP regulates the transition from replicative growth to stationary phase (180). *B. subtilis* requires proteolysis by ClpXP to initiate sporulation from mature to dead spores (182). Similar to Michalik *et al.* (69), we discovered that proteins involved in growth and reproduction (*e.g.*, ribosomal, translation, and cell wall synthesis proteins) were also regulated in a ClpP-dependent

manner. For example, ClpS, a ClpP chaperone, was observed to be upregulated at the RP in both the WT and Δ*clpP* strain, confirming that in the absence of ClpP, its chaperones can function as independent molecular chaperones (183–185) aside from enabling substrate entry into proteolytic chamber for ClpP-mediated degradation.

The signaling alarmone ppGpp is a key trigger for the stringent response in regulating *L. pneumophila* differentiation

(30, 33). *L. pneumophila* is equipped with two ppGpp syn-thetases, including RelA, which synthesizes ppGpp in response to fluctuations in amino acid availability, and the bifunctional enzyme SpoT, which controls the accumulation of ppGpp in response to fatty acid depletion (29, 115–117). Although previous reports have suggested a role for fatty acid signaling in the transition from the RP to the TP, the role of fatty acid signaling in the transition from the TP to the RP and the signaling protein(s) sensed by SpoT have not been re-ported. For example, in *E. coli*, there are numerous in-termediates/proteins in the fatty acid biosynthetic pathway; accordingly, more detailed studies are needed to determine which, if any, intermediate(s)/protein(s) triggers *L. pneumophila* differentiation *via* SpoT. Here, our data pro-vide the concrete evidence that fatty acid–related proteins Lpg0102, Lpg0361, and Lpg0362 play an important role in the transition from the TP to the RP by participating in the regu-lation of SpoT expression, which improve the completeness of the biphasic life cycle regulatory network between the RP and the TP. Our results also showed that the abundance of fatty acid synthesis–related proteins Lpg0102, Lpg0361, and Lpg0362 needs to be strictly regulated in a life stage–dependent manner (Fig. 4), corroborating the results of Aur-ass *et al.*, wherein these proteins were more abundant in the RP than the TP (14). We also confirmed that SpoT, but not RelA, responds to fatty acid signals and potentially plays a critical role during phase transition (29, 115). Dalebroux *et al.* (29) reported that only SpoT is required for *Legionella* prolif-eration in macrophages, and intracellular *L. pneumophila* uti-lizes SpoT in hydrolyzing ppGpp to reduce the alarmone pool and switch from the TP to the RP. Notably, we also observed that *spoT* expression is both temporal and ClpP dependent, suggesting the existence of a ClpP-mediated transcription regulator for *spoT*. We discovered that the ability of SpoT to sense variations in fatty acid metabolism and to activate the response to fluctuations in the lipid supply was also ClpP dependent. Furthermore, we found that Lpg0363 and LipB (Lpg1511) were direct substrates of ClpP, suggesting that ClpP may indirectly control Lpg0102, Lpg0361, Lpg0362, and SpoT *via* Lpg0363 and LipB. These data demonstrate that the ACP pathway may play a unique role in the life cycle of *L. pneumophila*. Hence, future research is needed to deter-mine the exact functions of the identified fatty acid synthesis proteins in *L. pneumophila* life cycle.

Several studies suggested that the control mechanism of biphasic life cycle and bacterial virulence of *L. pneumophila* is probably dependent. For example, RpoS regulates multiple pathways associated with motility and pathogenic functions and the activity of transcriptional regulators (19), LqsR, facili-tates the switch between the RP and TP (21), FliA is implicated in flagellum production (186), and CsrA activates replication traits and represses transmission traits (12). Similarly, *rpoS*, *lqsR*, *fliA*, and *csrA* are also required for the intracellular growth of *L. pneumophila* (12, 20, 21, 94). In specific, RpoS,

LqsR, FliA, and CsrA form a complex regulatory network that regulate the expression of more than 40 Dot/Icm effectors (17, 18, 21). The TCS protein PmrB interacts with its cognate response regulator PmrA, a protein required for *L. pneumophila* intracellular growth (104), creating PmrAB that activates the expression of 43 effector-encoding genes, positively regulates CsrA, and subsequently controls the post-transcriptional repression of CsrA-regulated effectors (17, 24). In this study, we discovered that the regulation of the biphasic life cycle and bacterial virulence is independent. Our findings also reveal that ClpP-mediated proteolysis regulates the expression of these regulatory proteins (*e.g.*, RpoS, LqsR, FliA, and CsrA) in a growth phase–dependent manner. On the other hand, we showed that the TCS protein PmrB is the substrate of ClpP, and PmrA is also regulated by ClpP. Compared with those of fatty acid biosynthesis–related pro-teins and CsrA (61), the ectopic expression of SpoT, an up-stream regulatory factor of RpoS, LqsR, PmrA, FliA, and CsrA, did not improve the proliferation ability of the Δ*clpP* strain in host cells (Fig. 7), although completely recovered the life cycle of the mutant (Fig. 6). Moreover, the temporal control of the synthesis and translocation of the effectors is required for *Legionella* to effectively manipulate the host cell pathways (40–45). The cyclic-di-GMP signaling is essential for the translocation of Dot/Icm effectors. For example, the presence of Lpg0744, a c-di-GMP-synthesizing enzyme, could modu-late the local pool of c-di-GMP near the Dot/Icm machinery, thus significantly contributing to the triggering of effector translocation (46). Remarkably, our proteomic data showed that the deletion of *clpP* affects the temporal expression of more than 120 effector proteins but does not reduce the expression level of Lpg0744, suggesting that the distinct temporal presence of these effector proteins might play important roles for functional assignments.

Surprisingly, at least 120 Dot/Icm effectors, some of which exhibit substantial effects on bacterial intracellular proliferation or trafficking in host cells, were observed to possess life stage–specific expression *via* ClpP regulation (Fig. 8). Among them, 53 effectors were also found in a previous report where 86 effectors were detected as differentially expressed in the RP and TP (14). The RP-specific proteins included PieF, Lpg2912, Ceg5, RavI, LegC4, YlfA, and MavM, whereas the TP-specific proteins consisted of VipD, RalF, LegC8, MavC, Lem7, LpnE, SdcA, SidC, SidM, SdeC, and SdeA. These data implied that the temporal control of Dot/Icm effector activity *via* ClpP-dependent proteolysis is required for the manipula-tion of the host cell pathways, in which the effectors poten-tially function at a specific life stage. Interestingly, several effectors that are important at specific phase of intracellular bacterial proliferation were also ClpP dependent. For example, LepA, which functions in release of the bacteria from amoebae at the TP and might not be needed at the RP, was more abundant at the RP in the Δ*clpP* strain than in the WT (127). VipD, which blocks endosome fusion with LCV, might be

needed at the TP and is immediately translocated into the host cytosol at the onset of infection and was less abundant at the TP in the Δ*clpP* strain than in the WT (151, 152). In contrast, the effectors required at the time of infection may have already accumulated in the TP and can be immediately delivered into the host cell. Correspondingly, the concentration of some effectors, such as SidC, SidJ, Lgt2, and RalF, was higher in the TP, suggesting that these are important at early stages of infection (49, 135, 154–156). Moreover, a proteomic analysis of the LCV at 1 h postinfection revealed a high overlap with the ClpP-regulated TP-specific effector proteins, including SdeA, LirA, Lpg1387, RavE, MavC, LegC6, Lpg2359, CegC4, Lem7, Lpg2844, LegC8, SidM/DrrA, Lpg2370, Lpg0279, SdeC, SidJ, Lem28, SidD, Lpg2327, RalF, SdcA, SidC, and Lpg2207 (187). This finding also indicated that ClpP-dependent proteolysis of effectors at a specific phase is required for *L. pneumophila* virulence. Our proteome data also showed that the levels of RavK, RavE, LirA, SdeC, Lpg2207, MavD, Lpg0279, LegA12, LpnE, and RalF were ClpP dependent at both the RP and TP, suggesting that their fine-tuned regulation might be vital for *L. pneumophila*. For example, LpnE is required for invasion and the establishment of an infection in macrophages, amoebae, and A/J mice (132–134), and RalF activates ADP-ribosylation factor on LCVs (49, 135). Surprisingly, DotU/IcmH was the only Dot/Icm protein complex that was identified as life stage specific and regulated *via* ClpP both at the RP and TP. As the inner membrane accessory factor, DotU/IcmH regulates the turnover of core components of Dot/Icm complex. The deletion of dotU/icmH leads to partial defects in intracellular growth and effector translocation (188, 189). Interestingly, DotU is one of the most widely distributed Dot/Icm proteins in many bacterial species that can interact with host cells but lacks a recognizable type IV secretion system (190). Thus, ClpP-dependent proteolysis is involved in the temporal regulation of Dot/Icm effectors and Dot/Icm core complex proteins; however, further research is required to elucidate the mechanisms underlying this process.

The ClpP^trap, a well-known system capable of capturing substrate proteins of ClpP, has been successfully utilized for *E. coli* and *S. aureus* (62, 170, 171). Thus, in this study, the capture of several validated ClpP substrates and unstable proteins in the ClpP^trap for *L. pneumophila* confirms that the proteins copurified with the ClpP^trap were genuine ClpP substrates. The substrate proteins were also associated with the pathways identified for the ClpP-dependent phase-specific regulatory proteins. For example, substrate protein MreC was known to be involved in cell division, whereas cell division proteins FtsA, FtsQ, FtsZ, and MreC were observed to have RP-specific expression. The substrate proteins PilZ, PilQ, and PilB were known to be involved in flagellar assembly, whereas the flagellar assembly–associated proteins MotA, FlgH, FlgI, FlgA, FlhF, Lpg0907, FliA, FliS, and PilM exhibited TP-specific expression. Thus, ClpP-dependent proteolysis can indirectly control cellular events by degrading pathway-associated

substrate proteins to regulate the abundance of controlled proteins. Notably, the abundance of several substrate proteins was observed to be both life stage specific and ClpP regulated. Hence, our data may help in understanding the mechanisms involved in the ClpP-mediated regulation of phase-specific regulatory proteins.

In conclusion, our study contributes a comprehensive insight into the temporal regulation of a large variety of differentially expressed proteins *via* ClpP-dependent proteolysis during the life cycle of *L. pneumophila*, demonstrating the significance of ClpP protease in the survival and virulence of this bacterial pathogen. Our findings also provide potential therapeutic targets for the development of antibacterial drugs against Legionnaires' disease in humans.

REFERENCES

1. Fields, B. S., Benson, R. F., and Besser, R. E. (2002) *Legionella* and Legionnaires' disease: 25 years of investigation. *Clin. Microbiol. Rev.* **15**, 506–526
2. Goncalves, I. G., Simoes, L. C., and Simoes, M. (2021) Legionella pneumophila. *Trends Microbiol.* **29**, 860–861
3. Rowbotham, T. J. (1980) Preliminary report on the pathogenicity of *Legionella pneumophila* for freshwater and soil amoebae. *J. Clin. Pathol.* **33**, 1179–1183
4. Newton, H. J., Ang, D. K., van Driel, I. R., and Hartland, E. L. (2010) Molecular pathogenesis of infections caused by *Legionella pneumophila*. *Clin. Microbiol. Rev.* **23**, 274–298
5. Chauhan, D., and Shames, S. R. (2021) Pathogenicity and Virulence of *Legionella*: Intracellular replication and host response. *Virulence* **12**, 1122–1144
6. Oliva, G., Sahr, T., and Buchrieser, C. (2018) The life cycle of *L. pneumophila*: Cellular differentiation is linked to virulence and metabolism. *Front. Cell Infect. Microbiol.* **8**, 3
7. Molofsky, A. B., and Swanson, M. S. (2004) Differentiate to thrive: Lessons from the *Legionella pneumophila* life cycle. *Mol. Microbiol.* **53**, 29–40
8. Byrne, B., and Swanson, M. S. (1998) Expression of *Legionella pneumophila* virulence traits in response to growth conditions. *Infect. Immun.* **66**, 3029–3034
9. Nora, T., Lomma, M., Gomez-Valero, L., and Buchrieser, C. (2009) Molecular mimicry: An important virulence strategy employed by *Legionella pneumophila* to subvert host functions. *Future Microbiol.* **4**, 691–701
10. Bruggemann, H., Hagman, A., Jules, M., Sismeiro, O., Dillies, M. A., Gouyette, C., Kunst, F., Steinert, M., Heuner, K., Coppee, J. Y., and Buchrieser, C. (2006) Virulence strategies for infecting phagocytes deduced from the *in vivo* transcriptional program of *Legionella pneumophila*. *Cell Microbiol.* **8**, 1228–1240
11. Faucher, S. P., Mueller, C. A., and Shuman, H. A. (2011) *Legionella pneumophila* transcriptome during intracellular multiplication in human macrophages. *Front. Microbiol.* **2**, 60
12. Molofsky, A. B., and Swanson, M. S. (2003) *Legionella pneumophila* CsrA is a pivotal repressor of transmission traits and activator of replication. *Mol. Microbiol.* **50**, 445–461
13. Hayashi, T., Nakamichi, M., Naitou, H., Ohashi, N., Imai, Y., and Miyake, M. (2010) Proteomic analysis of growth phase-dependent expression of *Legionella pneumophila* proteins which involves regulation of bacterial virulence traits. *PLoS One* **5**, e11718
14. Aurass, P., Gerlach, T., Becher, D., Voigt, B., Karste, S., Bernhardt, J., Riedel, K., Hecker, M., and Flieger, A. (2016) Life stage-specific proteomes of *Legionella pneumophila* reveal a highly differential abundance of virulence-associated dot/icm effectors. *Mol. Cell Proteomics* **15**, 177–200
15. Hauslein, I., Sahr, T., Escoll, P., Klausner, N., Eisenreich, W., and Buchrieser, C. (2017) *Legionella pneumophila* CsrA regulates a metabolic switch from amino acid to glycerolipid metabolism. *Open Biol.* **7**, 170149
16. McNealy, T. L., Forsbach-Birk, V., Shi, C., and Marre, R. (2005) The Hfq homolog in *Legionella pneumophila* demonstrates regulation by LetA and RpoS and interacts with the global regulator CsrA. *J. Bacteriol.* **187**, 1527–1532
17. Rasis, M., and Segal, G. (2009) The LetA-RsmYZ-CsrA regulatory cascade, together with RpoS and PmrA, post-transcriptionally regulates stationary phase activation of *Legionella pneumophila* Icm/Dot effectors. *Mol. Microbiol.* **72**, 995–1010
18. Sahr, T., Rusniok, C., Impens, F., Oliva, G., Sismeiro, O., Coppee, J. Y., and Buchrieser, C. (2017) The *Legionella pneumophila* genome evolved to accommodate multiple regulatory mechanisms controlled by the CsrA-system. *PLoS Genet.* **13**, e1006629
19. Bachman, M. A., and Swanson, M. S. (2004) Genetic evidence that *Legionella pneumophila* RpoS modulates expression of the transmission phenotype in both the exponential phase and the stationary phase. *Infect. Immun.* **72**, 2468–2476
20. Hales, L. M., and Shuman, H. A. (1999) The *Legionella pneumophila* rpoS gene is required for growth within *Acanthamoeba castellanii*. *J. Bacteriol.* **181**, 4879–4889
21. Tiaden, A., Spirig, T., Weber, S. S., Bruggemann, H., Bosshard, R., Buchrieser, C., and Hilbi, H. (2007) The *Legionella pneumophila* response regulator LqsR promotes host cell interactions as an element of the virulence regulatory network controlled by RpoS and LetA. *Cell Microbiol.* **9**, 2903–2920
22. Trigui, H., Dudyk, P., Oh, J., Hong, J. I., and Faucher, S. P. (2015) A regulatory feedback loop between RpoS and SpoT supports the survival of *Legionella pneumophila* in water. *Appl. Environ. Microbiol.* **81**, 918–928
23. Zusman, T., Gal-Mor, O., and Segal, G. (2002) Characterization of a *Legionella pneumophila* relA insertion mutant and toles of RelA and RpoS in virulence gene expression. *J. Bacteriol.* **184**, 67–75
24. Al-Khodor, S., Kalachikov, S., Morozova, I., Price, C. T., and Abu Kwaik, Y. (2009) The PmrA/PmrB two-component system of *Legionella pneumophila* is a global regulator required for intracellular replication within macrophages and protozoa. *Infect. Immun.* **77**, 374–386
25. Schulz, T., Rydzewski, K., Schunder, E., Holland, G., Bannert, N., and Heuner, K. (2012) FliA expression analysis and influence of the regulatory proteins RpoN, FleQ and FliA on virulence and *in vivo* fitness in *Legionella pneumophila*. *Arch. Microbiol.* **194**, 977–989
26. Morash, M. G., Brassinga, A. K., Warthan, M., Gourabathini, P., Garduno, R. A., Goodman, S. D., and Hoffman, P. S. (2009) Reciprocal expression of integration host factor and HU in the developmental cycle and infectivity of *Legionella pneumophila*. *Appl. Environ. Microbiol.* **75**, 1826–1837
27. Pitre, C. A. J., Tanner, J. R., Patel, P., and Brassinga, A. K. C. (2013) Regulatory control of temporally expressed integration host factor (IHF) in *Legionella pneumophila*. *Microbiology (Reading)* **159**, 475–492
28. Lynch, D., Fieser, N., Gloggler, K., Forsbach-Birk, V., and Marre, R. (2003) The response regulator LetA regulates the stationary-phase stress response in *Legionella pneumophila* and is required for efficient infection of *Acanthamoeba castellanii*. *FEMS Microbiol. Lett.* **219**, 241–248
29. Dalebroux, Z. D., Edwards, R. L., and Swanson, M. S. (2009) SpoT governs *Legionella pneumophila* differentiation in host macrophages. *Mol. Microbiol.* **71**, 640–658
30. Dalebroux, Z. D., Svensson, S. L., Gaynor, E. C., and Swanson, M. S. (2010) ppGpp conjures bacterial virulence. *Microbiol. Mol. Biol. Rev.* **74**, 171–199
31. Dalebroux, Z. D., and Swanson, M. S. (2012) ppGpp: magic beyond RNA polymerase. *Nat. Rev. Microbiol.* **10**, 203–212
32. Edwards, R. L., Jules, M., Sahr, T., Buchrieser, C., and Swanson, M. S. (2010) The *Legionella pneumophila* LetA/LetS two-component system exhibits rheostat-like behavior. *Infect. Immun.* **78**, 2571–2583
33. Hammer, B. K., and Swanson, M. S. (1999) Co-ordination of *legionella pneumophila* virulence with entry into stationary phase by ppGpp. *Mol. Microbiol.* **33**, 721–731
34. Hammer, B. K., Tateda, E. S., and Swanson, M. S. (2002) A two-component regulator induces the transmission phenotype of stationary-phase *Legionella pneumophila*. *Mol. Microbiol.* **44**, 107–118
35. Escoll, P., Mondino, S., Rolando, M., and Buchrieser, C. (2016) Targeting of host organelles by pathogenic bacteria: A sophisticated subversion strategy. *Nat. Rev. Microbiol.* **14**, 5–19
36. Hubber, A., and Roy, C. R. (2010) Modulation of host cell function by *Legionella pneumophila* type IV effectors. *Annu. Rev. Cell Dev. Biol.* **26**, 261–283
37. Isberg, R. R., O'Connor, T. J., and Heidtman, M. (2009) The *Legionella pneumophila* replication vacuole: Making a cosy niche inside host cells. *Nat. Rev. Microbiol.* **7**, 13–24
38. Qiu, J., and Luo, Z. Q. (2017) *Legionella* and *coxiella* effectors: Strength in diversity and activity. *Nat. Rev. Microbiol.* **15**, 591–605
39. He, L., Lin, Y., Ge, Z. H., He, S. Y., Zhao, B. B., Shen, D., He, J. G., and Lu, Y. J. (2019) The *Legionella pneumophila* effector WipA disrupts host F-actin polymerisation by hijacking phosphotyrosine signalling. *Cell Microbiol.* **21**, e13014
40. Liu, Y., Gao, P., Banga, S., and Luo, Z. Q. (2008) An *in vivo* gene deletion system for determining temporal requirement of bacterial virulence factors. *Proc. Natl. Acad. Sci. U. S. A.* **105**, 9385–9390
41. Neunuebel, M. R., Chen, Y., Gaspar, A. H., Backlund, P. S., Jr., Yergey, A., and Machner, M. P. (2011) De-AMPylation of the small GTPase Rab1 by the pathogen *Legionella pneumophila*. *Science* **333**, 453–456
42. Black, M. H., Osinski, A., Gradowski, M., Servage, K. A., Pawlowski, K., Tomchick, D. R., and Tagliabracci, V. S. (2019) Bacterial pseudokinase

catalyzes protein polyglutamylation to inhibit the SidE-family ubiquitin ligases. *Science* **364**, 787–792

43. Gan, N., Zhen, X., Liu, Y., Xu, X., He, C., Qiu, J., Liu, Y., Fujimoto, G. M., Nakayasu, E. S., Zhou, B., Zhao, L., Puvar, K., Das, C., Ouyang, S., and Luo, Z. Q. (2019) Regulation of phosphoribosyl ubiquitination by a calmodulin-dependent glutamylase. *Nature* **572**, 387–391

44. Bhogaraju, S., Bonn, F., Mukherjee, R., Adams, M., Pfleiderer, M. M., Galej, W. P., Matkovic, V., Lopez-Mosqueda, J., Kalayil, S., Shin, D., and Dikic, I. (2019) Inhibition of bacterial ubiquitin ligases by SidJ-calmodulin catalysed glutamylation. *Nature* **572**, 382–386

45. Sulpizio, A., Minelli, M. E., Wan, M., Burrowes, P. D., Wu, X., Sanford, E. J., Shin, J. H., Williams, B. C., Goldberg, M. L., Smolka, M. B., and Mao, Y. (2019) Protein polyglutamylation catalyzed by the bacterial calmodulin-dependent pseudokinase SidJ. *Elife* **8**, e51162

46. Allombert, J., Jaboulay, C., Michard, C., Andrea, C., Charpentier, X., Vianney, A., and Doublet, P. (2021) Deciphering *Legionella* effector delivery by Icm/Dot secretion system reveals a new role for c-di-GMP signaling. *J. Mol. Biol.* **433**, 166985

47. Bardill, J. P., Miller, J. L., and Vogel, J. P. (2005) IcmS-dependent translocation of SdeA into macrophages by the *Legionella pneumophila* type IV secretion system. *Mol. Microbiol.* **56**, 90–103

48. Luo, Z. Q., and Isberg, R. R. (2004) Multiple substrates of the *Legionella pneumophila* Dot/Icm system identified by interbacterial protein transfer. *Proc. Natl. Acad. Sci. U. S. A.* **101**, 841–846

49. Nagai, H., Kagan, J. C., Zhu, X., Kahn, R. A., and Roy, C. R. (2002) A bacterial guanine nucleotide exchange factor activates ARF on *Legionella* phagosomes. *Science* **295**, 679–682

50. Gottesman, S. (2003) Proteolysis in bacterial regulatory circuits. *Annu. Rev. Cell Dev. Biol.* **19**, 565–587

51. Mahmoud, S. A., and Chien, P. (2018) Regulated proteolysis in bacteria. *Annu. Rev. Biochem.* **87**, 677–696

52. Gur, E., Biran, D., and Ron, E. Z. (2011) Regulated proteolysis in Gram-negative bacteria–how and when? *Nat. Rev. Microbiol.* **9**, 839–848

53. Kahne, S. C., and Darwin, K. H. (2021) Structural determinants of regulated proteolysis in pathogenic bacteria by ClpP and the proteasome. *Curr. Opin. Struct. Biol.* **67**, 120–126

54. Konovalova, A., Sogaard-Andersen, L., and Kroos, L. (2014) Regulated proteolysis in bacterial development. *FEMS Microbiol. Rev.* **38**, 493–522

55. Wettstadt, S., and Llamas, M. A. (2020) Role of regulated proteolysis in the communication of bacteria with the environment. *Front. Mol. Biosci.* **7**, 586497

56. Becker, G., Klauck, E., and Hengge-Aronis, R. (1999) Regulation of RpoS proteolysis in *Escherichia coli*: The response regulator RssB is a recognition factor that interacts with the turnover element in RpoS. *Proc. Natl. Acad. Sci. U. S. A.* **96**, 6439–6444

57. Turgay, K., Hahn, J., Burghoorn, J., and Dubnau, D. (1998) Competence in *Bacillus subtilis* is controlled by regulated proteolysis of a transcription factor. *EMBO J.* **17**, 6730–6738

58. Zhou, Y., Gottesman, S., Hoskins, J. R., Maurizi, M. R., and Wickner, S. (2001) The RssB response regulator directly targets sigma(S) for degradation by ClpXP. *Genes Dev.* **15**, 627–637

59. Li, X. H., Zeng, Y. L., Gao, Y., Zheng, X. C., Zhang, Q. F., Zhou, S. N., and Lu, Y. J. (2010) The ClpP protease homologue is required for the transmission traits and cell division of the pathogen *Legionella pneumophila*. *BMC Microbiol.* **10**, 54

60. Zhao, B. B., Li, X. H., Zeng, Y. L., and Lu, Y. J. (2016) ClpP-deletion impairs the virulence of *Legionella pneumophila* and the optimal translocation of effector proteins. *BMC Microbiol.* **16**, 174

61. Ge, Z. H., Long, Q. S., Yuan, P. B., Pan, X., Shen, D., and Lu, Y. J. (2019) The temporal expression of global regulator protein CsrA is dually regulated by ClpP during the biphasic life cycle of *Legionella pneumophila*. *Front. Microbiol.* **10**, 2495

62. Feng, J., Michalik, S., Varming, A. N., Andersen, J. H., Albrecht, D., Jelsbak, L., Krieger, S., Ohlsen, K., Hecker, M., Gerth, U., Ingmer, H., and Frees, D. (2013) Trapping and proteomic identification of cellular substrates of the ClpP protease in *Staphylococcus aureus*. *J. Proteome Res.* **12**, 547–558

63. Feeley, J. C., Gibson, R. J., Gorman, G. W., Langford, N. C., Rasheed, J. K., Mackel, D. C., and Baine, W. B. (1979) Charcoal-yeast extract agar: Primary isolation medium for *Legionella pneumophila*. *J. Clin. Microbiol.* **10**, 437–441

64. Segal, G., and Shuman, H. A. (1999) *Legionella pneumophila* utilizes the same genes to multiply within *Acanthamoeba castellanii* and human macrophages. *Infect. Immun.* **67**, 2117–2124

65. Yuan, P., He, L., Chen, D., Sun, Y., Ge, Z., Shen, D., and Lu, Y. (2020) Proteomic characterization of *Mycobacterium tuberculosis* reveals potential targets of bostrycin. *J. Proteomics* **212**, 103576

66. Bernhardt, J., Funke, S., Hecker, M., and Siebourg, J. (2009) *Visualizing Gene Expression Data via Voronoi Treemaps,* Sixth International Symposium on Voronoi Diagrams. IEEE, Copenhagen. 233–241

67. Otto, A., Bernhardt, J., Meyer, H., Schaffer, M., Herbst, F. A., Siebourg, J., Mader, U., Lalk, M., Hecker, M., and Becher, D. (2010) Systems-wide temporal proteomic profiling in glucose-starved *Bacillus subtilis*. *Nat. Commun.* **1**, 137

68. Balzer, N., and Deussen, O. (2005) *Voronoi Treemaps,* Proceedings of the 2005 IEEE Symposium on Information Visualization. IEEE, Minneapolis, MN: 49–56

69. Michalik, S., Bernhardt, J., Otto, A., Moche, M., Becher, D., Meyer, H., Lalk, M., Schurmann, C., Schluter, R., Kock, H., Gerth, U., and Hecker, M. (2012) Life and death of proteins: A case study of glucose-starved *Staphylococcus aureus*. *Mol. Cell Proteomics* **11**, 558–570

70. Breiman, L. (2001) Random forests. *Machine Learn.* **45**, 5–32

71. *R: A Language and Environment for Statistical Computing in* R Foundation for Statistical Computing. (2018). R Core Team, Vienna

72. Al-Khodor, S., Price, C. T., Habyarimana, F., Kalia, A., and Abu Kwaik, Y. (2008) A Dot/Icm-translocated ankyrin protein of *Legionella pneumophila* is required for intracellular proliferation within human macrophages and protozoa. *Mol. Microbiol.* **70**, 908–923

73. Laemmli, U. K. (1970) Cleavage of structural proteins during the assembly of the head of bacteriophage T4. *Nature* **227**, 680–685

74. Towbin, H., Staehelin, T., and Gordon, J. (1979) Electrophoretic transfer of proteins from polyacrylamide gels to nitrocellulose sheets: Procedure and some applications. *Proc. Natl. Acad. Sci. U. S. A.* **76**, 4350–4354

75. Chien, M., Morozova, I., Shi, S., Sheng, H., Chen, J., Gomez, S. M., Asamani, G., Hill, K., Nuara, J., Feder, M., Rineer, J., Greenberg, J. J., Steshenko, V., Park, S. H., Zhao, B., *et al.* (2004) The genomic sequence of the accidental pathogen *Legionella pneumophila*. *Science* **305**, 1966–1968

76. Gillmaier, N., Schunder, E., Kutzner, E., Tlapak, H., Rydzewski, K., Herrmann, V., Stammler, M., Lasch, P., Eisenreich, W., and Heuner, K. (2016) Growth-related metabolism of the carbon storage poly-3-hydroxybutyrate in *Legionella pneumophila*. *J. Biol. Chem.* **291**, 6471–6482

77. Eisenreich, W., and Heuner, K. (2016) The life stage-specific pathometabolism of *Legionella pneumophila*. *FEBS Lett.* **590**, 3868–3886

78. Faulkner, G., and Garduno, R. A. (2002) Ultrastructural analysis of differentiation in *Legionella pneumophila*. *J. Bacteriol.* **184**, 7025–7041

79. Hughes, E. D., Byrne, B. G., and Swanson, M. S. (2019) A two-component system that modulates cyclic di-GMP metabolism promotes *Legionella pneumophila* differentiation and viability in low-nutrient conditions. *J. Bacteriol.* **201**, e00253-19

80. Zusman, T., Speiser, Y., and Segal, G. (2014) Two Fis regulators directly repress the expression of numerous effector-encoding genes in *Legionella pneumophila*. *J. Bacteriol.* **196**, 4172–4183

81. Edwards, R. L., Bryan, A., Jules, M., Harada, K., Buchrieser, C., and Swanson, M. S. (2013) Nicotinic acid modulates *Legionella pneumophila* gene expression and induces virulence traits. *Infect. Immun.* **81**, 945–955

82. Will, W. R., and Fang, F. C. (2020) The evolution of MarR family transcription factors as counter-silencers in regulatory networks. *Curr. Opin. Microbiol.* **55**, 1–8

83. Gupta, A., Pande, A., Sabrin, A., Thapa, S. S., Gioe, B. W., and Grove, A. (2019) MarR family transcription factors from *burkholderia* species: Hidden clues to control of virulence-associated genes. *Microbiol. Mol. Biol. Rev.* **83**, e00039-18

84. Grove, A. (2017) Regulation of metabolic pathways by MarR family transcription factors. *Comput. Struct. Biotechnol. J.* **15**, 366–371

85. Aurass, P., Prager, R., and Flieger, A. (2011) EHEC/EAEC O104:H4 strain linked with the 2011 German outbreak of haemolytic uremic syndrome enters into the viable but non-culturable state in response to various stresses and resuscitates upon stress relief. *Environ. Microbiol.* **13**, 3139–3148

86. Yu, M. J., Ren, J., Zeng, Y. L., Zhou, S. N., and Lu, Y. J. (2009) The *Legionella pneumophila* Dps homolog is regulated by iron and involved in multiple stress tolerance. *J. Basic Microbiol.* **49**, S79–S86

87. Quan, F. S., Kong, H. H., Lee, H. A., Chu, K. B., and Moon, E. K. (2020) Identification of differentially expressed *Legionella* genes during its intracellular growth in *Acanthamoeba. Heliyon* **6**, e05238

88. Ohnishi, Y., Yamazaki, H., Kato, J. Y., Tomono, A., and Horinouchi, S. (2005) AdpA, a central transcriptional regulator in the A-factor regulatory cascade that leads to morphological development and secondary metabolism in *Streptomyces griseus. Biosci. Biotechnol. Biochem.* **69**, 431–439

89. Ueguchi, C., Kakeda, M., Yamada, H., and Mizuno, T. (1994) An analogue of the DnaJ molecular chaperone in *Escherichia coli. Proc. Natl. Acad. Sci. U. S. A.* **91**, 1054–1058

90. Chae, C., Sharma, S., Hoskins, J. R., and Wickner, S. (2004) CbpA, a DnaJ homolog, is a DnaK co-chaperone, and its activity is modulated by CbpM. *J. Biol. Chem.* **279**, 33147–33153

91. Sarraf, N. S., Shi, R., McDonald, L., Baardsnes, J., Zhang, L., Cygler, M., and Ekiel, I. (2014) Structure of CbpA J-domain bound to the regulatory protein Cbpm explains its specificity and suggests evolutionary link between Cbpm and transcriptional regulators. *PLoS One* **9**, e100441

92. Fatima, K., Naqvi, F., and Younas, H. (2021) A review: Molecular chaperone-mediated folding, unfolding and disaggregation of expressed recombinant proteins. *Cell Biochem. Biophys.* **79**, 153–174

93. Eraso, J. M., Markillie, L. M., Mitchell, H. D., Taylor, R. C., Orr, G., and Margolin, W. (2014) The highly conserved MraZ protein is a transcriptional regulator in *Escherichia coli. J. Bacteriol.* **196**, 2053–2066

94. Hochstrasser, R., and Hilbi, H. (2017) Intra-species and inter-kingdom signaling of *Legionella pneumophila. Front. Microbiol.* **8**, 79

95. Hochstrasser, R., Hutter, C. A. J., Arnold, F. M., Barlocher, K., Seeger, M. A., and Hilbi, H. (2020) The structure of the *Legionella* response regulator LqsR reveals amino acids critical for phosphorylation and dimerization. *Mol. Microbiol.* **113**, 1070–1084

96. Personnic, N., Striednig, B., Lezan, E., Manske, C., Welin, A., Schmidt, A., and Hilbi, H. (2019) Quorum sensing modulates the formation of virulent *Legionella* persisters within infected cells. *Nat. Commun.* **10**, 5216

97. Schell, M. A. (1993) Molecular biology of the LysR family of transcriptional regulators. *Annu. Rev. Microbiol.* **47**, 597–626

98. Maddocks, S. E., and Oyston, P. C. F. (2008) Structure and function of the LysR-type transcriptional regulator (LTTR) family proteins. *Microbiology (Reading)* **154**, 3609–3623

99. Ueta, M., Yoshida, H., Wada, C., Baba, T., Mori, H., and Wada, A. (2005) Ribosome binding proteins YhbH and YfiA have opposite functions during 100S formation in the stationary phase of *Escherichia coli. Genes Cells* **10**, 1103–1112

100. Maki, Y., Yoshida, H., and Wada, A. (2000) Two proteins, YfiA and YhbH, associated with resting ribosomes in stationary phase *Escherichia coli. Genes Cells* **5**, 965–974

101. Padilla-Vaca, F., Mondragon-Jaimes, V., and Franco, B. (2017) General aspects of two-component regulatory circuits in bacteria: Domains, signals and roles. *Curr. Protein Pept. Sci.* **18**, 990–1004

102. Gal-Mor, O., and Segal, G. (2003) Identification of CpxR as a positive regulator of icm and dot virulence genes of *Legionella pneumophila. J. Bacteriol.* **185**, 4908–4919

103. Gal-Mor, O., and Segal, G. (2003) The *Legionella pneumophila* GacA homolog (LetA) is involved in the regulation of *icm* virulence genes and is required for intracellular multiplication in *Acanthamoeba castellanii. Microb. Pathog.* **34**, 187–194

104. Zusman, T., Aloni, G., Halperin, E., Kotzer, H., Degtyar, E., Feldman, M., and Segal, G. (2007) The response regulator PmrA is a major regulator of the *icm/dot* type IV secretion system in *Legionella pneumophila* and *Coxiella burnetii. Mol. Microbiol.* **63**, 1508–1523

105. Altman, E., and Segal, G. (2008) The response regulator CpxR directly regulates expression of several *Legionella pneumophila* icm/dot components as well as new translocated substrates. *J. Bacteriol.* **190**, 1985–1996

106. Chatterjee, D., Boyd, C. D., O'Toole, G. A., and Sondermann, H. (2012) Structural characterization of a conserved, calcium-dependent periplasmic protease from *Legionella pneumophila. J. Bacteriol.* **194**, 4415–4425

107. Chatterjee, D., Cooley, R. B., Boyd, C. D., Mehl, R. A., O'Toole, G. A., and Sondermann, H. (2014) Mechanistic insight into the conserved allosteric regulation of periplasmic proteolysis by the signaling molecule cyclic-di-GMP. *Elife* **3**, e03650

108. Jacobi, S., Schade, R., and Heuner, K. (2004) Characterization of the alternative sigma factor sigma54 and the transcriptional regulator FleQ of *Legionella pneumophila*, which are both involved in the regulation cascade of flagellar gene expression. *J. Bacteriol.* **186**, 2540–2547

109. Lenn, T., Leake, M. C., and Mullineaux, C. W. (2008) Clustering and dynamics of cytochrome bd-I complexes in the *Escherichia coli* plasma membrane *in vivo. Mol. Microbiol.* **70**, 1397–1407

110. Mason, M. G., Shepherd, M., Nicholls, P., Dobbin, P. S., Dodsworth, K. S., Poole, R. K., and Cooper, C. E. (2009) Cytochrome bd confers nitric oxide resistance to *Escherichia coli. Nat. Chem. Biol.* **5**, 94–96

111. Appelt, S., and Heuner, K. (2017) The flagellar regulon of *legionella*-A review. *Front. Cell Infect. Microbiol.* **7**, 454

112. Albert-Weissenberger, C., Sahr, T., Sismeiro, O., Hacker, J., Heuner, K., and Buchrieser, C. (2010) Control of flagellar gene regulation in *Legionella pneumophila* and its relation to growth phase. *J. Bacteriol.* **192**, 446–455

113. Heuner, K., Dietrich, C., Skriwan, C., Steinert, M., and Hacker, J. (2002) Influence of the alternative sigma(28) factor on virulence and flagellum expression of *Legionella pneumophila. Infect. Immun.* **70**, 1604–1608

114. Bachman, M. A., and Swanson, M. S. (2004) The LetE protein enhances expression of multiple LetA/LetS-dependent transmission traits by *Legionella pneumophila. Infect. Immun.* **72**, 3284–3293

115. Edwards, R. L., Dalebroux, Z. D., and Swanson, M. S. (2009) *Legionella pneumophila* couples fatty acid flux to microbial differentiation and virulence. *Mol. Microbiol.* **71**, 1190–1204

116. Battesti, A., and Bouveret, E. (2006) Acyl carrier protein/SpoT interaction, the switch linking SpoT-dependent stress response to fatty acid metabolism. *Mol. Microbiol.* **62**, 1048–1063

117. Xiao, H., Kalman, M., Ikehara, K., Zemel, S., Glaser, G., and Cashel, M. (1991) Residual guanosine 3',5'-bispyrophosphate synthetic activity of *relA* null mutants can be eliminated by spoT null mutations. *J. Biol. Chem.* **266**, 5980–5990

118. Potrykus, K., and Cashel, M. (2008) ppGpp: still magical? *Annu. Rev. Microbiol.* **62**, 35–51

119. Joshi, A. D., Sturgill-Koszycki, S., and Swanson, M. S. (2001) Evidence that Dot-dependent and -independent factors isolate the *Legionella pneumophila* phagosome from the endocytic network in mouse macrophages. *Cell Microbiol.* **3**, 99–114

120. Losick, V. P., Haenssler, E., Moy, M. Y., and Isberg, R. R. (2010) LnaB: A *Legionella pneumophila* activator of NF-kappaB. *Cell Microbiol.* **12**, 1083–1097

121. Belyi, Y., Jank, T., and Aktories, K. (2013) Cytotoxic glucosyltransferases of *Legionella pneumophila. Curr. Top. Microbiol. Immunol.* **376**, 211–226

122. Belyi, Y. (2020) Targeting eukaryotic mRNA translation by *Legionella pneumophila. Front. Mol. Biosci.* **7**, 80

123. Wang, Y., Shi, M., Feng, H., Zhu, Y., Liu, S., Gao, A., and Gao, P. (2018) Structural insights into non-canonical ubiquitination catalyzed by SidE. *Cell* **173**, 1231–1243.e16

124. Puvar, K., Luo, Z. Q., and Das, C. (2019) Uncovering the structural basis of a new twist in protein ubiquitination. *Trends Biochem. Sci.* **44**, 467–477

125. Toulabi, L., Wu, X., Cheng, Y., and Mao, Y. (2013) Identification and structural characterization of a *Legionella* phosphoinositide phosphatase. *J. Biol. Chem.* **288**, 24518–24527

126. Li, G., Liu, H., Luo, Z. Q., and Qiu, J. (2021) Modulation of phagosome phosphoinositide dynamics by a *Legionella* phosphoinositide 3-kinase. *EMBO Rep.* **22**, e51163

127. Chen, J., de Felipe, K. S., Clarke, M., Lu, H., Anderson, O. R., Segal, G., and Shuman, H. A. (2004) *Legionella* effectors that promote nonlytic release from protozoa. *Science* **303**, 1358–1361

128. Chen, J., Reyes, M., Clarke, M., and Shuman, H. A. (2007) Host cell-dependent secretion and translocation of the LepA and LepB effectors of *Legionella pneumophila. Cell Microbiol.* **9**, 1660–1671

129. Finsel, I., Ragaz, C., Hoffmann, C., Harrison, C. F., Weber, S., van Rahden, V. A., Johannes, L., and Hilbi, H. (2013) The *Legionella* effector RidL inhibits retrograde trafficking to promote intracellular replication. *Cell Host Microbe* **14**, 38–50

130. de Felipe, K. S., Glover, R. T., Charpentier, X., Anderson, O. R., Reyes, M., Pericone, C. D., and Shuman, H. A. (2008) *Legionella* eukaryotic-like type IV substrates interfere with organelle trafficking. *PLoS Pathog.* **4**, e1000117

131. Degtyar, E., Zusman, T., Ehrlich, M., and Segal, G. (2009) A *Legionella* effector acquired from protozoa is involved in sphingolipids metabolism and is targeted to the host cell mitochondria. *Cell Microbiol.* **11**, 1219–1235

132. Newton, H. J., Sansom, F. M., Bennett-Wood, V., and Hartland, E. L. (2006) Identification of *Legionella pneumophila*-specific genes by genomic subtractive hybridization with *Legionella micdadei* and identification of *lpnE*, a gene required for efficient host cell entry. *Infect. Immun.* **74**, 1683–1691

133. Newton, H. J., Sansom, F. M., Dao, J., McAlister, A. D., Sloan, J., Cianciotto, N. P., and Hartland, E. L. (2007) Sel1 repeat protein LpnE is a *Legionella pneumophila* virulence determinant that influences vacuolar trafficking. *Infect. Immun.* **75**, 5575–5585

134. Weber, S. S., Ragaz, C., and Hilbi, H. (2009) The inositol polyphosphate 5-phosphatase OCRL1 restricts intracellular growth of *Legionella*, localizes to the replicative vacuole and binds to the bacterial effector LpnE. *Cell Microbiol.* **11**, 442–460

135. Nagai, H., Cambronne, E. D., Kagan, J. C., Amor, J. C., Kahn, R. A., and Roy, C. R. (2005) A C-terminal translocation signal required for Dot/Icm-dependent delivery of the *Legionella* RalF protein to host cells. *Proc. Natl. Acad. Sci. U. S. A.* **102**, 826–831

136. Bennett, T. L., Kraft, S. M., Reaves, B. J., Mima, J., O'Brien, K. M., and Starai, V. J. (2013) LegC3, an effector protein from *Legionella pneumophila*, inhibits homotypic yeast vacuole fusion *in vivo* and *in vitro*. *PLoS One* **8**, e56798

137. Yao, D., Cherney, M., and Cygler, M. (2014) Structure of the N-terminal domain of the effector protein LegC3 from *Legionella pneumophila*. *Acta Crystallogr. D Biol. Crystallogr.* **70**, 436–441

138. Choy, A., Dancourt, J., Mugo, B., O'Connor, T. J., Isberg, R. R., Melia, T. J., and Roy, C. R. (2012) The *Legionella* effector RavZ inhibits host autophagy through irreversible Atg8 deconjugation. *Science* **338**, 1072–1076

139. Wong, K., Kozlov, G., Zhang, Y., and Gehring, K. (2015) Structure of the *Legionella* effector, lpg1496, suggests a role in nucleotide metabolism. *J. Biol. Chem.* **290**, 24727–24737

140. Belyi, I., Popoff, M. R., and Cianciotto, N. P. (2003) Purification and characterization of a UDP-glucosyltransferase produced by *Legionella pneumophila*. *Infect. Immun.* **71**, 181–186

141. Belyi, Y., Tabakova, I., Stahl, M., and Aktories, K. (2008) Lgt: A family of cytotoxic glucosyltransferases produced by *Legionella pneumophila*. *J. Bacteriol.* **190**, 3026–3035

142. Hurtado-Guerrero, R., Zusman, T., Pathak, S., Ibrahim, A. F., Shepherd, S., Prescott, A., Segal, G., and van Aalten, D. M. (2010) Molecular mechanism of elongation factor 1A inhibition by a *Legionella pneumophila* glycosyltransferase. *Biochem. J.* **426**, 281–292

143. Lu, W., Du, J., Stahl, M., Tzivelekidis, T., Belyi, Y., Gerhardt, S., Aktories, K., and Einsle, O. (2010) Structural basis of the action of glucosyltransferase Lgt1 from *Legionella pneumophila*. *J. Mol. Biol.* **396**, 321–331

144. Urbanus, M. L., Quaile, A. T., Stogios, P. J., Morar, M., Rao, C., Di Leo, R., Evdokimova, E., Lam, M., Oatway, C., Cuff, M. E., Osipiuk, J., Michalska, K., Nocek, B. P., Taipale, M., Savchenko, A., *et al*. (2016) Diverse mechanisms of metaeffector activity in an intracellular bacterial pathogen, *Legionella pneumophila*. *Mol. Syst. Biol.* **12**, 893

145. Liu, Y., Zhu, W., Tan, Y., Nakayasu, E. S., Staiger, C. J., and Luo, Z. Q. (2017) A *Legionella* effector disrupts host cytoskeletal structure by cleaving actin. *PLoS Pathog.* **13**, e1006186

146. Xu, L., Shen, X., Bryan, A., Banga, S., Swanson, M. S., and Luo, Z. Q. (2010) Inhibition of host vacuolar H+-ATPase activity by a *Legionella pneumophila* effector. *PLoS Pathog.* **6**, e1000822

147. Zhao, J., Beyrakhova, K., Liu, Y., Alvarez, C. P., Bueler, S. A., Xu, L., Xu, C., Boniecki, M. T., Kanelis, V., Luo, Z. Q., Cygler, M., and Rubinstein, J. L. (2017) Molecular basis for the binding and modulation of V-ATPase by a bacterial effector protein. *PLoS Pathog.* **13**, e1006394

148. Derre, I., and Isberg, R. R. (2005) LidA, a translocated substrate of the *Legionella pneumophila* type IV secretion system, interferes with the early secretory pathway. *Infect. Immun.* **73**, 4370–4380

149. Cheng, W., Yin, K., Lu, D., Li, B., Zhu, D., Chen, Y., Zhang, H., Xu, S., Chai, J., and Gu, L. (2012) Structural insights into a unique *Legionella pneumophila* effector LidA recognizing both GDP and GTP bound Rab1 in their active state. *PLoS Pathog.* **8**, e1002528

150. Bugalhao, J. N., Mota, L. J., and Franco, I. S. (2016) Identification of regions within the *Legionella pneumophila* VipA effector protein involved in actin binding and polymerization and in interference with eukaryotic organelle trafficking. *Microbiologyopen* **5**, 118–133

151. Ku, B., Lee, K. H., Park, W. S., Yang, C. S., Ge, J., Lee, S. G., Cha, S. S., Shao, F., Heo, W. D., Jung, J. U., and Oh, B. H. (2012) VipD of *Legionella pneumophila* targets activated Rab5 and Rab22 to interfere with endosomal trafficking in macrophages. *PLoS Pathog.* **8**, e1003082

152. Gaspar, A. H., and Machner, M. P. (2014) VipD is a Rab5-activated phospholipase A1 that protects *Legionella pneumophila* from endosomal fusion. *Proc. Natl. Acad. Sci. U. S. A.* **111**, 4560–4565

153. Lucas, M., Gaspar, A. H., Pallara, C., Rojas, A. L., Fernandez-Recio, J., Machner, M. P., and Hierro, A. (2014) Structural basis for the recruitment and activation of the *Legionella* phospholipase VipD by the host GTPase Rab5. *Proc. Natl. Acad. Sci. U. S. A.* **111**, E3514–E3523

154. Ragaz, C., Pietsch, H., Urwyler, S., Tiaden, A., Weber, S. S., and Hilbi, H. (2008) The *Legionella pneumophila* phosphatidylinositol-4 phosphate-binding type IV substrate SidC recruits endoplasmic reticulum vesicles to a replication-permissive vacuole. *Cell Microbiol.* **10**, 2416–2433

155. Horenkamp, F. A., Mukherjee, S., Alix, E., Schauder, C. M., Hubber, A. M., Roy, C. R., and Reinisch, K. M. (2014) *Legionella pneumophila* subversion of host vesicular transport by SidC effector proteins. *Traffic* **15**, 488–499

156. Hsu, F., Luo, X., Qiu, J., Teng, Y. B., Jin, J., Smolka, M. B., Luo, Z. Q., and Mao, Y. (2014) The *Legionella* effector SidC defines a unique family of ubiquitin ligases important for bacterial phagosomal remodeling. *Proc. Natl. Acad. Sci. U. S. A.* **111**, 10538–10543

157. Tan, Y., and Luo, Z. Q. (2011) *Legionella pneumophila* SidD is a deAMPylase that modifies Rab1. *Nature* **475**, 506–509

158. Chen, Y., Tascon, I., Neunuebel, M. R., Pallara, C., Brady, J., Kinch, L. N., Fernandez-Recio, J., Rojas, A. L., Machner, M. P., and Hierro, A. (2013) Structural basis for Rab1 de-AMPylation by the *Legionella pneumophila* effector SidD. *PLoS Pathog.* **9**, e1003382

159. Machner, M. P., and Isberg, R. R. (2006) Targeting of host Rab GTPase function by the intravacuolar pathogen *Legionella pneumophila*. *Dev. Cell* **11**, 47–56

160. Machner, M. P., and Isberg, R. R. (2007) A bifunctional bacterial protein links GDI displacement to Rab1 activation. *Science* **318**, 974–977

161. Murata, T., Delprato, A., Ingmundson, A., Toomre, D. K., Lambright, D. G., and Roy, C. R. (2006) The *Legionella pneumophila* effector protein DrrA is a Rab1 guanine nucleotide-exchange factor. *Nat. Cell Biol.* **8**, 971–977

162. Brombacher, E., Urwyler, S., Ragaz, C., Weber, S. S., Kami, K., Overduin, M., and Hilbi, H. (2009) Rab1 guanine nucleotide exchange factor SidM is a major phosphatidylinositol 4-phosphate-binding effector protein of *Legionella pneumophila*. *J. Biol. Chem.* **284**, 4846–4856

163. Ninio, S., Zuckman-Cholon, D. M., Cambronne, E. D., and Roy, C. R. (2005) The *Legionella* IcmS-IcmW protein complex is important for Dot/Icm-mediated protein translocation. *Mol. Microbiol.* **55**, 912–926

164. Liu, Y., and Luo, Z. Q. (2007) The *Legionella pneumophila* effector SidJ is required for efficient recruitment of endoplasmic reticulum proteins to the bacterial phagosome. *Infect. Immun.* **75**, 592–603

165. Lin, Y. H., Doms, A. G., Cheng, E., Kim, B., Evans, T. R., and Machner, M. P. (2015) Host cell-catalyzed S-palmitoylation mediates golgi targeting of the *Legionella* ubiquitin ligase GobX. *J. Biol. Chem.* **290**, 25766–25781

166. Ledvina, H. E., Kelly, K. A., Eshraghi, A., Plemel, R. L., Peterson, S. B., Lee, B., Steele, S., Adler, M., Kawula, T. H., Merz, A. J., Skerrett, S. J., Celli, J., and Mougous, J. D. (2018) A phosphatidylinositol 3-kinase effector alters phagosomal maturation to promote intracellular growth of *francisella*. *Cell Host Microbe* **24**, 285–295.e8

167. Kubori, T., and Nagai, H. (2016) The type IVB secretion system: An enigmatic chimera. *Curr. Opin. Microbiol.* **29**, 22–29

168. Nagai, H., and Kubori, T. (2011) Type IVB secretion systems of *Legionella* and other gram-negative bacteria. *Front. Microbiol.* **2**, 136

169. Berger, K. H., Merriam, J. J., and Isberg, R. R. (1994) Altered intracellular targeting properties associated with mutations in the *Legionella pneumophila* dotA gene. *Mol. Microbiol.* **14**, 809–822

170. Flynn, J. M., Neher, S. B., Kim, Y. I., Sauer, R. T., and Baker, T. A. (2003) Proteomic discovery of cellular substrates of the ClpXP protease reveals five classes of ClpX-recognition signals. *Mol. Cell* **11**, 671–683

171. Neher, S. B., Villen, J., Oakes, E. C., Bakalarski, C. E., Sauer, R. T., Gygi, S. P., and Baker, T. A. (2006) Proteomic profiling of ClpXP substrates after DNA damage reveals extensive instability within SOS regulon. *Mol. Cell* **22**, 193–204

172. Frees, D., Qazi, S. N., Hill, P. J., and Ingmer, H. (2003) Alternative roles of ClpX and ClpP in *Staphylococcus aureus* stress tolerance and virulence. *Mol. Microbiol.* **48**, 1565–1578

173. Frees, D., Chastanet, A., Qazi, S., Sorensen, K., Hill, P., Msadek, T., and Ingmer, H. (2004) Clp ATPases are required for stress tolerance, intracellular replication and biofilm formation in *Staphylococcus aureus*. *Mol. Microbiol.* **54**, 1445–1462

174. Frees, D., Andersen, J. H., Hemmingsen, L., Koskenniemi, K., Baek, K. T., Muhammed, M. K., Gudeta, D. D., Nyman, T. A., Sukura, A., Varmanen, P., and Savijoki, K. (2012) New insights into *Staphylococcus aureus* stress tolerance and virulence regulation from an analysis of the role of the ClpP protease in the strains Newman, COL, and SA564. *J. Proteome Res.* **11**, 95–108

175. Chattoraj, P., Banerjee, A., Biswas, S., and Biswas, I. (2010) ClpP of *Streptococcus* mutans differentially regulates expression of genomic islands, mutacin production, and antibiotic tolerance. *J. Bacteriol.* **192**, 1312–1323

176. Zheng, J., Wu, Y., Lin, Z., Wang, G., Jiang, S., Sun, X., Tu, H., Yu, Z., and Qu, D. (2020) ClpP participates in stress tolerance, biofilm formation, antimicrobial tolerance, and virulence of *Enterococcus faecalis*. *BMC Microbiol.* **20**, 30

177. Camberg, J. L., Hoskins, J. R., and Wickner, S. (2009) ClpXP protease degrades the cytoskeletal protein, FtsZ, and modulates FtsZ polymer dynamics. *Proc. Natl. Acad. Sci. U. S. A.* **106**, 10614–10619

178. Camberg, J. L., Hoskins, J. R., and Wickner, S. (2011) The interplay of ClpXP with the cell division machinery in *Escherichia coli*. *J. Bacteriol.* **193**, 1911–1918

179. Williams, B., Bhat, N., Chien, P., and Shapiro, L. (2014) ClpXP and ClpAP proteolytic activity on divisome substrates is differentially regulated following the *Caulobacter asymmetric* cell division. *Mol. Microbiol.* **93**, 853–866

180. Hengge, R. (2009) Proteolysis of sigmaS (RpoS) and the general stress response in *Escherichia coli*. *Res. Microbiol.* **160**, 667–676

181. Joshi, K. K., and Chien, P. (2016) Regulated proteolysis in bacteria: *Caulobacter*. *Annu. Rev. Genet.* **50**, 423–445

182. Tan, I. S., Weiss, C. A., Popham, D. L., and Ramamurthi, K. S. (2015) A quality-control mechanism removes unfit cells from a population of sporulating bacteria. *Dev. Cell* **34**, 682–693

183. Savijoki, K., Ingmer, H., and Varmanen, P. (2006) Proteolytic systems of lactic acid bacteria. *Appl. Microbiol. Biotechnol.* **71**, 394–406

184. Frees, D., Savijoki, K., Varmanen, P., and Ingmer, H. (2007) Clp ATPases and ClpP proteolytic complexes regulate vital biological processes in low GC, Gram-positive bacteria. *Mol. Microbiol.* **63**, 1285–1295

185. Frees, D., Brondsted, L., and Ingmer, H. (2013) Bacterial proteases and virulence. *Subcell Biochem.* **66**, 161–192

186. Heuner, K., Hacker, J., and Brand, B. C. (1997) The alternative sigma factor sigma28 of *Legionella pneumophila* restores flagellation and motility to an *Escherichia coli fliA* mutant. *J. Bacteriol.* **179**, 17–23

187. Hoffmann, C., Finsel, I., Otto, A., Pfaffinger, G., Rothmeier, E., Hecker, M., Becher, D., and Hilbi, H. (2014) Functional analysis of novel Rab GTPases identified in the proteome of purified *Legionella*-containing vacuoles from macrophages. *Cell Microbiol.* **16**, 1034–1052

188. VanRheenen, S. M., Dumenil, G., and Isberg, R. R. (2004) IcmF and DotU are required for optimal effector translocation and trafficking of the *Legionella pneumophila* vacuole. *Infect. Immun.* **72**, 5972–5982

189. Sexton, J. A., Miller, J. L., Yoneda, A., Kehl-Fie, T. E., and Vogel, J. P. (2004) *Legionella pneumophila* DotU and IcmF are required for stability of the Dot/Icm complex. *Infect. Immun.* **72**, 5983–5992

190. Das, S., Chakrabortty, A., Banerjee, R., Roychoudhury, S., and Chaudhuri, K. (2000) Comparison of global transcription responses allows identification of *Vibrio cholerae* genes differentially expressed following infection. *FEMS Microbiol. Lett.* **190**, 87–91

191. Ma, J., Chen, T., Wu, S., Yang, C., Bai, M., Shu, K., Li, K., Zhang, G., Jin, Z., He, F., Hermjakob, H., and Zhu, Y. (2019) iProX: an integrated proteome resource. *Nucleic Acids Res.* **47**, D1211–D1217